STUDY OF THE KINETICS OF THE HYDROSILYLATION REACTION: ITS ROLE AND STATE OF THE ART

F. D. Krylov,*[a] K. A. Bezlepkina,[a,b] S. A. Milenin,[a,b] and A. M. Muzafarov[a,c]

[a] Enikolopov Institute of Synthetic Polymeric Materials, Russian Academy of Sciences, ul. Profsoyuznaya 70, Moscow, 117393 Russia
[b] Research Laboratory of New Silicone Materials and Technologies, Tula State Lev Tolstoy Pedagogical University, pr. Lenina 125, Tula, Tula Oblast, 300026 Russia
[c] Nesmeyanov Institute of Organoelement Compounds, Russian Academy of Sciences, ul. Vavilova 28, str. 1, Moscow, 119334 Russia

Abstract

Silicones are one of the most important materials, without which it is difficult to imagine human life in the 21st century. Hydrosilylation is widely used to obtain functional silanes and siloxanes. This review summarizes the available data on the kinetics of the interaction of silyl hydrides in the composition of different molecules with various alkenyl substrates under the hydrosilylation reaction conditions.

Key words: hydrosilylation, allylsiloxanes, allylsilanes, vinyl, vinylsiloxanes, vinylsilanes, platinum, siloxanes, kinetics, Karstedt's catalyst.
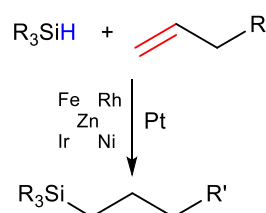
1. Introduction

Silicones are one of the most important materials, without which it is difficult to imagine human life in the 21st century. They feature a number of unique properties, such as low glass transition temperature, excellent thermal and oxidative stability, high gas permeability, prominent dielectric properties, good wettability of the processed surface, low temperature dependence of physical properties, physiological inertness, biocompatibility, as well as the possibility of easy functionalization [1–5]. All these allowed silicones to become widespread in almost all areas of our life and in most industries: construction and transport engineering, household chemicals and cosmetics, transport and agriculture [6–8]. Silicones are widely used in electrical engineering and electronics [9], drug delivery systems [10], implants [11], antifouling, anticorrosive coatings [12, 13], and other areas [14, 15]. A broad spectrum of silicone applications requires a wide variety of materials with clearly defined structures and properties. The most important role in obtaining such siloxane-based materials is played by vulcanization reactions (cross-linking, curing), which imply the formation of cross-linked three-dimensional network structures. Controlling the reactions of network structure formation is of high importance for the properties of materials and the economics of such processes.

Nowadays, a wide range of synthetic approaches are used for the synthesis of cross-linked polyorganosiloxanes with a given structure, which include the following polycondensation reactions: hydrosilylation, thiol–ene addition, click reactions in general, and others [16–23].

Perhaps the hydrosilylation reaction has received the greatest significance and popularity in the field of modification and vulcanization of silicones. The hydrosilylation process is widely used in the synthesis of industrially used organofunctional silanes, as well as in the production of important reagents for organic synthesis [24]. In particular, hydrosilylation is commonly utilized as a commercially important method for cross-linking silicone rubbers as well as organic polymers containing vinyl or allyl groups with siloxanes and polysiloxanes bearing a Si–H bond [25]. Many interesting new materials, in particular polycarbosilanes, can be obtained by the hydrosilylation method [26–29]. In addition, hydrosilylation reactions are used for the functionalization of oligo(poly)siloxanes featuring Si–H bonds for the synthesis of silicon-containing dendrimers [30–33], as well as for the functionalization of silsesquioxanes and their use as nanofillers in the synthesis of modern nanomaterials [34, 35].

As for silicone rubbers, they are classified according to the curing mechanism and conditions. According to their curing conditions, silicone rubbers are mainly divided into two groups of materials: room temperature vulcanizing (RTV) and high temperature vulcanizing (HTV) (hard silicone rubbers).

A new group of materials designed for processing in injection molding machines appeared about 20–30 years ago. Due to their low viscosity and pasty behavior, they were called liquid silicone rubbers (LSRs) or simply liquid rubbers (LRs) [36, 37].

Hydrosilylation is finding increasing application in the production of silicone rubbers owing to many technological and economic advantages [38], as evidenced by its involvement in large-scale chemical production and a plethora of reviews on the investigations of this reaction [25, 39].

An important parameter for the production of elastomeric silicone materials is the reaction kinetics, which allows for achieving reproducible and finely tuned properties of the resulting materials. This is especially important for the curing of silicones [40–43], 3D printing [44–47] and coating processes [48, 49].

The reaction kinetics is also important to study for the optimization of the process conditions, for example, in organic synthesis, analytical reactions, and chemical production [50, 51]. This latter example is an important aspect of chemical engineering. Kinetic data are also used to determine and control the stability of commercial products, such as pharmaceutical formulations, food products, paints, and metals. Some further applications of kinetics, less extensive than the mentioned ones, include testing of the rate theories, measuring equilibrium constants, analyzing solutions, in particular, mixtures of dissolved substances, and defining the solvent properties that depend on the reaction rates [52–5]. The most versatile and therefore most common process used in silicone vulcanization is hydrosilylation. This review is devoted to the investigations on the kinetics of this process.

More specifically, the goal of this review was to highlight the currently available information on the kinetics of the interaction of silyl hydrides in the composition of different molecules with various alkenyl substrates under the hydrosilylation reaction conditions.

2. Hydrosilylation reaction

Hydrosilylation reactions are widely used to obtain functional silanes and siloxanes. Hydrosilylation is a term that describes the addition reaction of organic and inorganic silicon hydrides to different types of unsaturated functional groups, in particular, carbon–carbon and carbon–heteroatom (*i.e.*, carbon–oxygen and carbon–nitrogen), as well as heteroatom–heteroatom (*e.g.*, nitrogen–nitrogen and nitrogen–oxygen) bonds. In catalytic transformations of organosilicon compounds, hydrosilylation is a well-known process dominating in industrial applications [56]. However, it should be noted that there are other reactions for the production of functional siloxanes, such as the catalytic rearrangement of low molecular weight siloxanes [17] or the thiol–ene polyaddition reaction [21], which are gaining popularity as the methods for synthesis and functionalization in the chemistry of organosilicon polymers and individual compounds. Despite the active development of these processes, the predominance of hydrosilylation reactions in industrially important processes of silicone chemistry is currently undeniable.

The first mention of the hydrosilylation reaction refers to 1947, when an octene molecule was added to trichlorosilane in the presence of a peroxide catalyst [25]. The first report on Speier's platinum catalyst dates back to 1957 (almost 70 years ago) [25], and the first application of the hydrosilylation reaction in polymer science dates back to 1967 (according to a Web of Science research). At present, a large number of articles and reviews on this topic have been published and the number of reports in the field continues to grow every year [16, 24, 25, 56–63].

The types of polymers and materials synthesized by hydrosilylation can be divided into four broad classes:

(A) linear comb-like polymers;

(B) dendritic/hyperbranched systems or framework materials;

(C) siloxane or organic polymers functionalized by hydrosilylation;

(D) linear polymers containing mainly silicon and carbon atoms (and sometimes other atoms) in the backbone, many of them are s–p conjugated systems.

However, this classification is rather conditional. Frameworks can be outlined as a separate group, while the separation of siloxane polymers from the general structural classification is not justified. It is more correct to operate with the general classification of polymers by the chain structure (linear, branched, network) with the addition of molecular nanoobjects. Nevertheless, there are only few studies on the kinetics of hydrosilylation of polymers, so this review deals with the kinetics of hydrosilylation primarily of individual model compounds.

3. Kinetics of the hydrosilylation reaction over platinum catalysts

Catalytic hydrosilylation has been studied using a number of metals, namely Pt, Pd, Ni, Rh, Ir, Co, Fe, and Ru. Nowadays, most hydrosilylation reactions in industry are carried out using so-called Speier's (H_2PtCl_6) and Karstedt's catalysts. The main advantages of these catalysts are their selectivity, high reaction rates, and amenability to regeneration [16, 71]. Based on the study of phosphine complexes of Pt(II) and Ir(I), a mechanism of hydrosilylation of alkenes (by analogy with hydrogenation) was proposed, which was called the Chalk–Harrod mechanism (Scheme 1) [59].
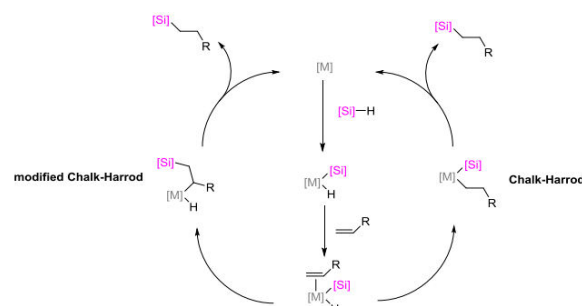
Scheme 1. Chalk–Harrod mechanism and modified Chalk–Harrod mechanism.

As can be seen from Scheme 1 (a right part), the first stage involves the oxidative addition of silicon hydride $HSiR_3$ to the platinum catalyst, then the alkene is coordinated with the intermediate and is inserted into the Pt–H bond. Subsequently, the reductive elimination by the Si–C bond takes place. Both the oxidative addition of the hydrosilane to the platinum catalyst, accompanied by the olefin coordination, and the coordination of the olefin with the platinum catalyst, accompanied by the oxidative addition of the hydrosilane, are possible. There have been attempts to study intermediates formed during hydrosilylation; however, their exact structures have not been established yet. The Chalk–Harrod mechanism does not explain such phenomena as the appearance of an induction period in the case of some catalysts, as well as the formation of vinylsilanes. Therefore, the modified Chalk–Harrod mechanism was proposed (a left part of Scheme 1), according to which the olefin is inserted into the Pt–Si bond, and the reductive elimination occurs by the C–H bond. According to both the original and

modified versions of the Chalk–Harrod mechanism, the platinum group metal catalysts should be able to break the Si–H bond, weaken the C=C bond upon the olefin coordination, and be resistant to the reduction to the metal [64–66].

The investigations on the kinetics of hydrosilylation were conducted back in the early 2000s. Thus, Stein *et al.* [67] studied the mechanism of hydrosilylation using highly active Karstedt's precatalyst ($Pt_x(M^{vinyl}M^{vinyl})_y$, $M^{vinyl}M^{vinyl}$. The work was carried out using the extended X-ray absorption fine structure (EXAFS) method, small-angle X-ray scattering (SAXS), and UV spectroscopy.

The authors determined the period of time during which the reaction proceeded most rapidly using gas chromatographic analysis. Then the reactions were repeated, and the solutions were frozen in liquid nitrogen during the most active part of the catalytic cycle for the EXAFS analysis. The EXAFS analysis of the frozen solutions revealed the presence of Pt–C (2.18 Å) and Pt–Si (2.32 Å) bonds with a Pt–C to Pt–Si ratio of about 3:1 and the absence of Pt–Pt bonds. Thus, according to the authors, the main part of platinum exists as mononuclear species during the hydrosilylation reaction, regardless of the nature of the reactants or stoichiometry.

Figure 1 shows the results of the preliminary kinetic experiments performed using GC, from which a number of trends became apparent. At stoichiometric excess of the hydrosilane, a certain increase in the rate is observed, consistent with the positive dependence of the rate on the hydrosilane concentration and the inverse dependence on the olefin concentration. However, the kinetic studies performed using gas chromatography, where the samples were subjected to poorly controlled temperature impact, can significantly distort the reliability of the experimental results.
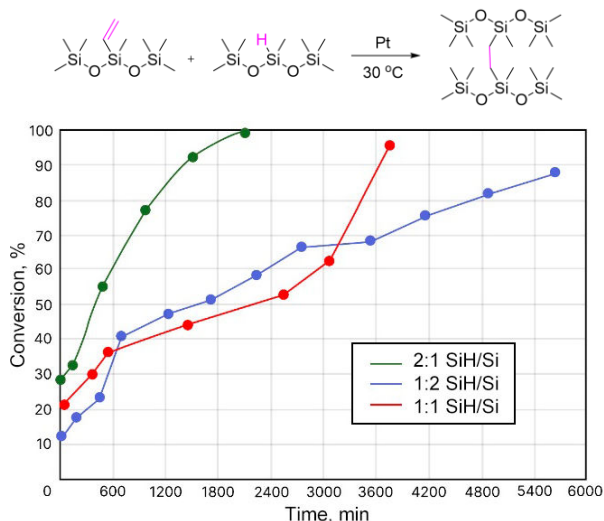

Figure 1. Reaction of MDViM with MDHM at different stoichiometric ratios. The results were obtained using GC [67].

These investigations showed that, regardless of the stoichiometric ratio of the hydrosilane and olefin, the catalyst is a monomeric compound of platinum with silicon and carbon in the first coordination sphere. However, the final platinum product depends on the stoichiometry of the reactants. An explanation of the oxygen effect was also given. In the absence of oxygen, hydrosilylation of some olefins does not occur.

Oxygen promotes the destruction of polynuclear platinum particles that are formed in the case of poorly stabilizing olefins.

Cancouët *et al.* [68] considered the kinetics of hydrosilylation of allyloxy-2,3-epoxypropane (allyl glycidyl ether, AGE) with poly(hydrogenmethylsiloxane-co-dimethylsiloxane)s (D^H-D copolymers) of various compositions, followed by the production of polysiloxanes containing epoxy groups as side substituents. Hexachloroplatinic acid was used as a catalyst.

The kinetic studies were performed using IR spectroscopy. After taking samples, they were cooled with ice to completely stop the reaction. The studies were carried out with a PHMS sample with M_n = 58000 in toluene at 70 °C. When introducing the catalyst into a solution containing equimolar amounts of the silane functions and AGE, an induction period was observed and the reaction rate gradually increased, as is shown in Fig. 2.
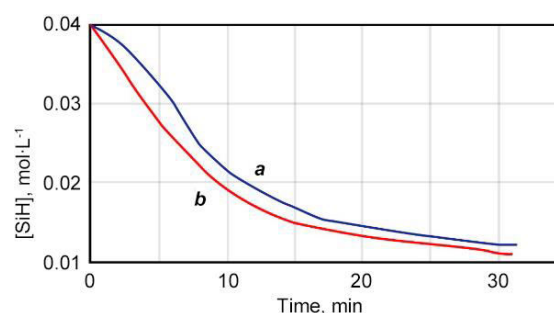

Figure 2. Induction period during hydrosilylation of AGE using PHMS: all reagents are mixed (time t = 0) (***a***), AGE and H_2PtCl_6 are in contact for 20 min before the addition of PHMS (***b***). $[SiH]_0$ = 0.04 mol·L^{-1}; $[AGE]_0$ = 0.04 mol·L^{-1}; $[H_2PtCl_6]$ = 1.25·10^{-5} mol·L^{-1}; T = 70 °C; the solvent was toluene.

The kinetic order by platinum was determined by plotting the logarithm of the initial rate of silane consumption (R_0) *vs.* the logarithm of $[Pt]_0$ (Fig. 3). The initial order in the silane functions was determined from the logarithmic plot of R_0 as a function of the initial concentration ($[SiH]_0$) (Fig. 4). This order was equal to 0.5. The external order in the double bonds was determined analogously.
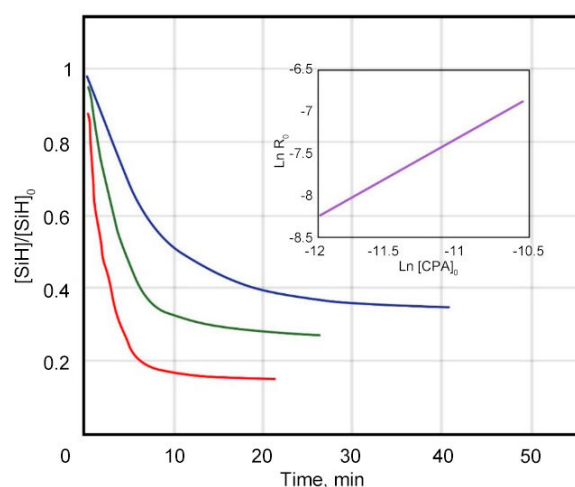

Figure 3. Effect of the concentration of H_2PtCl_6 on the rate of hydrosilylation. $[SiH]_0$ = 0.25 mol·L^{-1}; $[AGE]_0$ = 0.25 mol·L^{-1}; T = 70 °C; the solvent was toluene; $[H_2PtCl_6]$ = 6.25 10^{-6} mol·L^{-1} (blue curve), 1.25 10^{-5} mol·L^{-1} (green curve), and 2.5 10^{-5} mol·L^{-1} (red curve).
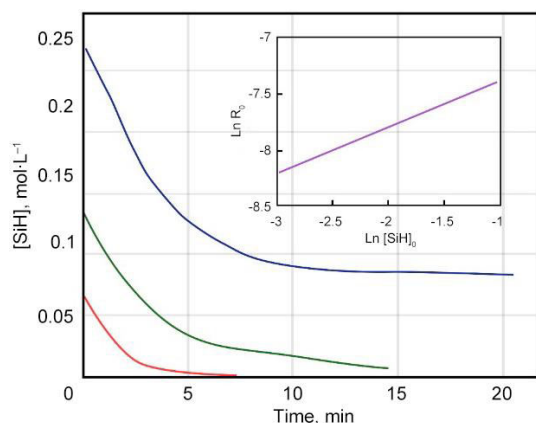
Figure 4. Effect of the concentration of the silane functions on the rate of hydrosilylation. $[AGE]_0 = 0.25$ mol·L^{-1}; $[H_2PtCl_6] = 1.25·10^{-5}$ mol·L^{-1}; $T = 70$ °C; the solvent was toluene; $[SiH] = 0.245$ mol·L^{-1} (blue curve), 0.122 mol·L^{-1} (green curve), and 0 (red curve).

The change in R_0 depending on the concentration of the double bonds (always used in excess with respect to the initial concentration of the silane) indicated the first order with respect to the allyl groups. Hence, these measurements are consistent with the hypothesis that hydrogenmethylsiloxane dyads are much more reactive than the isolated units, which can be explained by the simultaneous introduction of two vicinal Si–H bonds into the binuclear platinum complex.

Taking this into account, we can conclude that the hydrosilylation rate can be presented by the following equation

$$-\frac{d[SiH]}{dt} = k[Pt]^1[SiH]^{0.5}[AGE]^1$$

The kinetic order by the silane was unexpected and rarely observed in monosilanes. Therefore, the authors suggested that the proximity of several silane groups in the PHMS sequence may explain this observation. Since the olefin–platinum structures exist mainly as binuclear complexes, it can be assumed that two platinum atoms are able to interact with two adjacent silane functions in the polymer. Such a geometry may explain why two hydrosilylation products were formed for one activated species. This suggestion is consistent with a reaction scheme similar to that proposed by Chalk and Harrod.

The authors assumed that bimetallic addition product HPt$_2$Si is significantly less reactive than monometallic addition product HPtSi. Consequently, in the absence of adjacent Si–H bonds, hydrosilylation proceeds very slowly.

Hence, the performed kinetic studies showed that PHMS and its copolymers display a peculiar behavior, which can be called the neighbor effect, consisting in the fact that the hydrogenmethylsiloxane unit is much more reactive when it has an adjacent hydrogenmethylsiloxane unit than when it is isolated between two dialkyl-substituted siloxane moieties. From a practical point of view, the low reactivity of isolated silane groups requires the use of more severe conditions to achieve the complete conversion. This is especially important for the copolymers with a low content of units. However, to reach the quantitative conversion in a short period of time, it seems reasonable to significantly increase the temperature.

de Vekki *et al.* [69] explored the rate of addition of MeSiH(OSiMe$_3$)$_2$, Me$_2$SiHOSiMe$_3$, and (Me$_2$SiH)$_2$O to vinylsiloxanes Vi(Me)Si(OSiMe$_3$)$_2$, Vi(Me)$_2$SiOSiMe$_3$, and (Vi(Me)$_2$Si)$_2$O in the presence of platinum complexes.

Disiloxanes Me$_2$SiHOSiMe$_3$ and ViMe$_2$SiOSiMe$_3$ were considered as the models of polymers with a terminal hydrogen atom and a vinyl group, and trisiloxanes MeSiH(OSiMe$_3$)$_2$ and ViMeSi(OSiMe$_3$)$_2$—as the models with the above-mentioned functional groups in the side chain. According to the authors, the most interesting system was monomeric system (Me$_2$SiH)$_2$O–(ViMe$_2$Si)$_2$O, in which each component has two active groups. All platinum(II) sulfoxide complexes at a concentration of 10–35 M appeared to be effective catalysts for hydrosilylation in siloxane systems at 20–60 °C. The kinetics of the process was monitored using GLC.

The analysis of the kinetic data on catalytic hydrosilylation of siloxanes showed that the reactivity of vinylsiloxanes and siloxysilicon hydrides strongly depends on the electronic and steric properties of substituents at a silicon atom. At an equimolar ratio of the reagents in the presence of platinum(II) sulfoxide complexes, the following reactivity series was obtained: (Me$_2$SiH)$_2$O >> Me$_2$SiHOSiMe$_3$ > MeSiH(OSiMe$_3$)$_2$. This series corresponds to an increase in the positive charge on a silicon atom, which promotes strengthening of the Si–H bond. In addition, on passing from (Me$_2$SiH)$_2$O to MeSiH(OSiMe$_3$)$_2$, the contribution of the steric factor also increases, providing a further decrease in the reactivity of MeSiH(OSiMe$_3$)$_2$ relative to disiloxanes (Table 1).

Table 1. Hydrosilylation of tetramethyldivinyldisiloxane with excess tetramethyldisiloxane in the presence of *cis*-Pt(Et$_2$SO)$_2$Cl$_2$ ($c_0 = 10^{-5}$ M)

Reaction time, min	Conversion, %	Selectivity, %			
		β,β-adduct	α,α-adduct	β,α-adduct	A,β-adduct
60	100	57.5	–	42.5	–
90	100	46.8	3.5	38.5	11.2
150	100	48.3	4.6	41.0	16.1
210	100	41.5	5.5	36.3	16.7
270	100	50.0	11.1	30.5	8.4
300	100	39.9	8.7	36.0	15.4
360	83	36.6	14.3	30.1	19.0
420	86	47.8	19.9	26.3	6.3
540	90	59.5	8.3	25.2	7.1
600	91	53.1	8.2	33.3	5.3

In the presence of *bis*-sulfoxide and mixed sulfoxide–pyridine Pt(II) complexes, the reactivity of vinylsiloxanes (at an equimolar ratio of the reagents) changes in parallel with a decrease in the electron density on the silicon atom to which the vinyl group is attached. The reactivity of the second vinyl group in (ViMe$_2$Si)$_2$O is difficult to estimate due to the simultaneous hydrosilylation of both double bonds, but at a ratio of 3-divinylsiloxane to 3-monovinylsiloxane of 2:1, the rate of the addition of one vinylsiloxane group in the monovinylsiloxane system is higher.

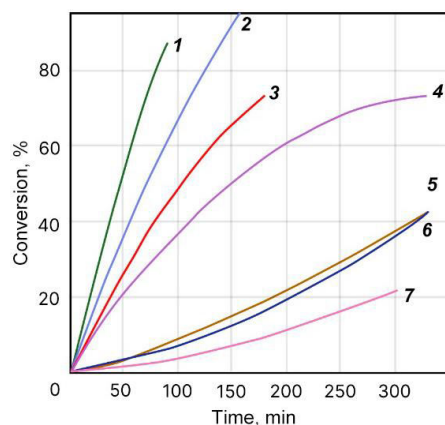Thus, the reactivity series of vinylsiloxanes in the hydrosilylation reaction follows graphs in Fig. 5.

Figure 5. Changes in the conversion of the vinyl substrate during hydrosilylation in the presence of *cis*-[Pt(MeSO-Tol-*p*)(Py)Cl$_2$] (25 °C, $c_0 = 10^{-4}$ M) in the following systems: ViMeSi(OSiMe$_3$)$_2$–(Me$_2$SiH)$_2$O (*1*), ViMe$_2$SiOSiMe$_3$–Me$_2$SiHOSiMe$_3$ (*2*),ViMeSi(OSiMe$_3$)$_2$–Me$_2$SiHOSiMe$_3$ (*3*), ViMe$_2$SiOSiMe$_3$–MeSiH(OSiMe$_3$)$_2$ (*4*), (ViMe$_2$Si)$_2$O–(Me$_2$SiH)$_2$O (*5*), (ViMe$_2$Si)$_2$–3Me$_2$SiHOSiMe$_3$ (*6*), and ViMeSi(OSiMe$_3$)$_2$–MeSiH(OSiMe$_3$)$_2$ (1:1) (*7*).

Thus, the work represented the investigations on the kinetics of hydrosilylation of a fairly wide range of model compounds in the presence of platinum complexes as catalysts. The conclusions about the reactivity of these catalysts were outlined. Varying X with an unchanged ligand L and L' leads to a decrease in the reaction rate in the following series: C$_2$O$_4^{2-}$ > NO$_3^-$ > Cl$^-$ >> Br$^-$. Heteroligand complexes such as (–)-[Pt(MeSOTol-*p*)PyCl$_2$] having a *cis*-structure are more effective catalysts for hydrosilylation of siloxanes than the corresponding *trans*-isomers. The reactions of platinum(II) sulfoxide complexes with vinylsiloxanes and silicon hydrides lead to the isomerization of the metal complex and dissociation of the sulfoxide ligand; the *bis*-sulfoxide complexes undergo deoxygenation of the sulfoxide ligand to form colloidal platinum. However, it should be noted that the kinetic measurements were carried out by GLC, which may cause uncertainties in the form of uncontrolled heating of the samples, as was in Ref. [67].

Marciniec *et al.* [70] investigated the kinetics of substrate transformations in industrially important hydrosilylation of allyl chloride with trichlorosilane catalyzed by platinum applied to activated carbon (Scheme 2) as well as the yields of the main product (3-chloropropyltrichlorosilane) and side products (tetrachlorosilane, propyltrichlorosilane). The course of the reaction was monitored using GC.
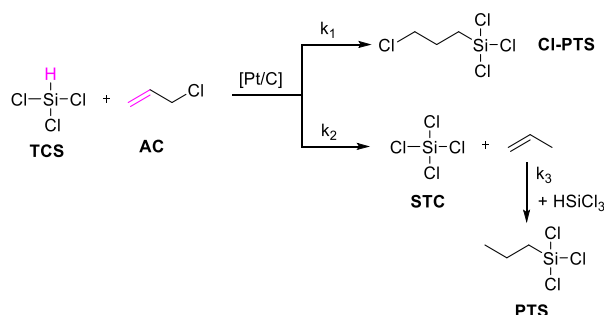
Most of the experiments were carried out using a slight excess of HSiCl$_3$ (1.1–1.2:1.0). The excess is probably necessary because of the occurrence of a side reaction (with the release of propene) at the competitive stage of H/Cl exchange. However, the reaction order with respect to both substrates was determined based on the experiments carried out with a 3:1 excess of specific substrates. Both sets of the experiments indicated good agreement with the pseudo-first-order dependence of the secondary substrate consumption. At the same time, a pseudo-first-order dependence of the overall reaction rate constant k_{obs} (calculated from the substrate consumption) was also found at the equimolar concentrations of both substrates (Fig. 6).
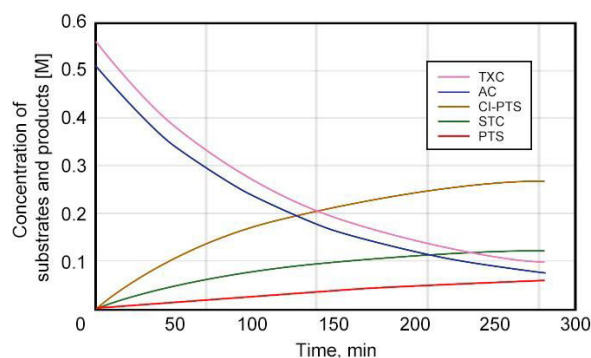

Figure 6. Examples of the kinetic curves.

Qiong and Hong in a small study [71] examined the kinetics of hydrosilylation of unsaturated allyl polyether bearing a terminal ester group with polyhydrosiloxane. Chloroplatinic acid was used as a catalyst, and ethyl acetate was used as a solvent to eliminate mass transfer resistance in the system.

The kinetics of the reaction was studied using liquid chromatography. The authors characterized the rate of conversion with respect to the polyether by the ratio of the area of the first peak to that of two peaks. However, the original chromatograms are missing in the work, which reduces the value of the resulting data.

At the mass ratio of all reactants to the solvent equal to 1:4, the catalyst concentration is $1.5 \cdot 10^{-4}$ mol/L (Pt), the molar ratio of the Si–H bonds to the carbon–carbon double bonds is 1 to 1.3, the curve of the polyether conversion over time was obtained at four different temperatures. In Fig. 7, the straight lines do not pass through the starting point due to the existence of an induction period. From the kinetic dependences depicted in Fig. 8, the rate constants at different temperatures were estimated.
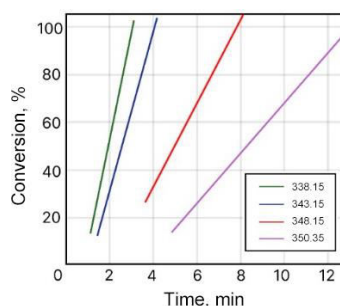

Scheme 2. Stepwise hydrosilylation of allyl chloride with trichlorosilane.

Figure 7. Conversion of the polyether at four different temperatures.
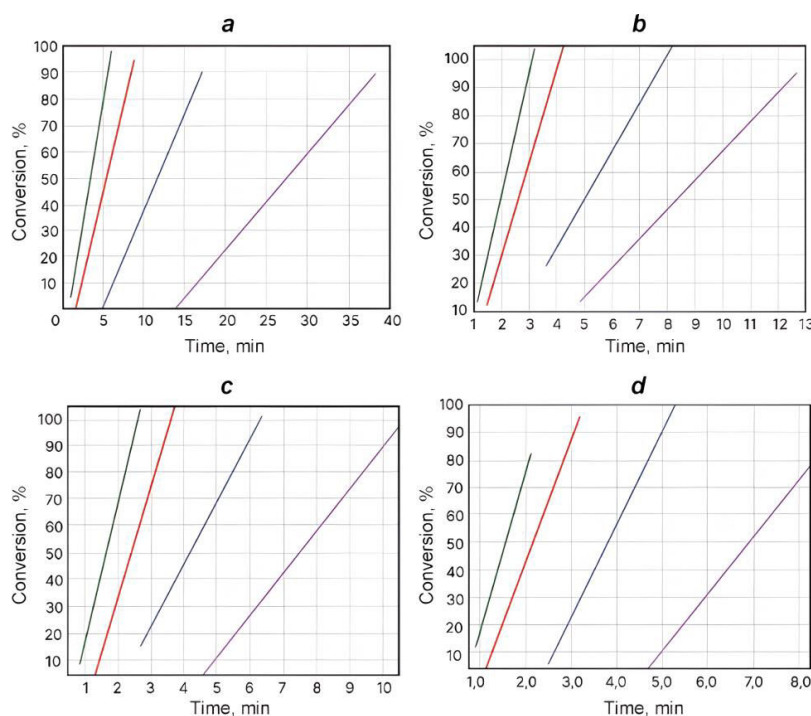
Figure 8. Time dependences: $c_{cat} = 1.0 \cdot 10^{-4}$ mol·L^{-1}, Pt (*a*); $c_{cat} = 1.5 \cdot 10^{-4}$ mol·L^{-1}, Pt (*b*); $c_{cat} = 2.3 \cdot 10^{-4}$ mol·L^{-1}, Pt (*c*); $c_{cat} = 3.1 \cdot 10^{-4}$ mol·L^{-1}, Pt (*d*).

As a result, it was found that the model parameters change linearly depending on the catalyst concentration. The kinetics of the reaction between polyhydrosiloxane and allyl polyether is important for the production of siloxane–oxyalkylene copolymers, which are widely used in different fields of industry owing to their high surface activity.

Imlinger *et al.* [72] reported the hydrosilylation reaction performed in the presence of platinum(II) dichloride as a catalyst and 1,1,3,3-tetramethyldisiloxane and divinylbenzene as reagents (Scheme 3). The reaction was monitored in real time using Fourier-transform infrared (FTIR) spectroscopy, and the kinetics was determined using self-modeling curve resolution (SMCR). This system is similar to hydrosilylation of styrene with triethylsilane using the same platinum precursor. The authors aimed at defining whether a simple catalyst PtCl$_2$ can be used to prepare poly[1,1,3,3-tetramethyl-1-(ethylenephenyleneethylene)disiloxane]$_4$ and to show the superiority of the multivariate approach to the kinetic analysis even when the kinetic model under study is simple and analytically resolvable.
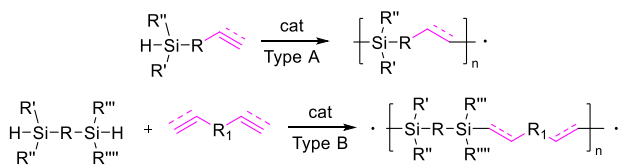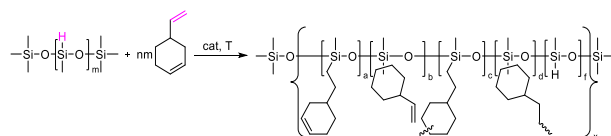

Scheme 3. Scheme of the hydrosilylation reaction for polymerization in general.

According to the authors, the silicon hydride band at 2100 cm^{-1} is not suitable for the quantitative analysis, since there is a strong background absorption in the same region from diamond used as the attenuated total reflection (ATR) material. The fingerprint region shows a change in the peak intensity with potentially clean peak profiles of a single component. A careful inspection of the adduct and solvent spectra suggested that the bands at 878 cm^{-1} (assigned to Si–H bending) and 988 cm^{-1} (assigned to vinyl CH$_2$ vibrations) may be suitable for univariate analysis. In the authors' opinion, IR spectroscopy is not very sensitive to double bonds; therefore, the signal at 988 cm^{-1} is low and, due to potential overlapping with the adjacent siloxane band, is not suitable for the kinetic measurements, although this statement was not indicated.

Mukbaniani *et al.* [73] studied the synthesis of polysiloxanes with side unsaturated cyclic moieties, which was accomplished by hydrosilylation of 4-vinyl-1-cyclohexene with polymethylhydrosiloxane in the presence of a platinum catalyst (Scheme 4). The reactions were carried out at different temperatures with different ratios of the starting compounds.

Scheme 4. Hydrosilylation of 4-vinyl-1-cyclohexene with a,x-*bis*(trimethylsiloxy)methylhydrosiloxane.

The authors noted that, without a solvent, the reaction proceeds vigorously, and at the initial stages of the conversion of Si–H bonds (30%), the gelation occurs. To prevent this and to study the kinetic parameters, the reaction was carried out in toluene.

The structures and compositions of the oligomers were established using elemental and functional analysis, FTIR spectra, ^{1}H, ^{13}C, ^{1}H–^{1}H COSY, and ^{1}H–^{13}C NMR correlation spectra.

Figure 9 shows that at 40 °C the hydrosilylation reaction proceeds with a conversion of active Si–H groups of 75%, while at 60 °C, the hydrosilylation reaction proceeds with a conversion of 91%. Consequently, an increase in the temperature leads to an

increase in the conversion of active Si–H groups. It is known from the literature that hydrosilylation reactions, as usual at the initial stages, have the second order at the stoichiometric ratio of the starting compounds relative to Si–H bonds. According to the results of the experiments, an increase in the concentration of one of the reactants does not change the reaction order.
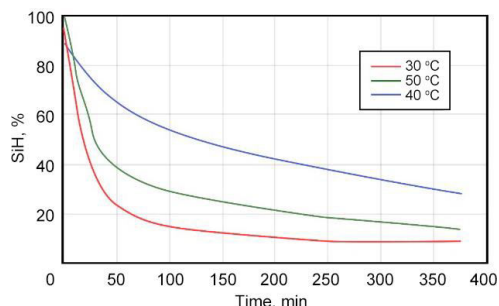

Figure 9. Dependence of the change in the concentration of active Si–H groups on time during the hydrosilylation of 4-vinyl-1-cyclohexene with a,x-*bis*(trimethylsiloxy)methylhydrosiloxane at different temperatures (H$_2$PtCl$_6$, ratio 1:70).

The hydrosilylation reactions of 4-vinyl-1-cyclohexene with PMHS in the presence of Speier's catalyst (0.1 M in THF) at different ratios of the starting compounds were analyzed. At a stoichiometric ratio of 1:3 for Si–H bonds, the reaction proceeded with a conversion of active Si–H bonds of 92%. At a ratio of 1:4 for Si–H bonds, the conversion of active Si–H bonds was 99%.

The comparison was carried out under optimal reaction conditions: for H$_2$PtCl$_6$ and Karstedt's catalysts, it was 60 °C, while for Pt/C, it was 100 °C. However, in the presence of Pt/C at 60 °C the reaction did not proceed. The effect of the catalysts on the reaction rate and the conversion of active Si–H groups was clearly shown. It can be concluded that the activity of the catalysts of hydrosilylation of 4-vinyl-1-cyclohexene with PMHS decreases in the following series: H$_2$PtCl$_6$ > Karstedt's catalyst > Pt/C (Fig. 10).
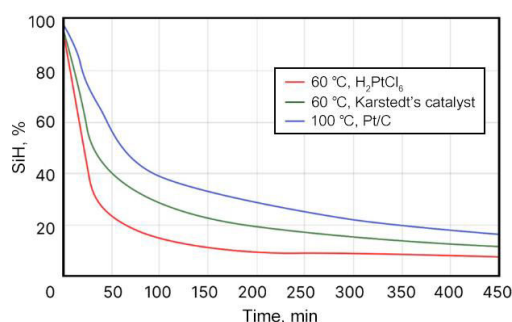

Figure 10. Dependence of the change in the concentration of active Si–H groups on time during the hydrosilylation of 4-vinyl-1-cyclohexene with a,x-*bis*(trimethylsiloxy)methylhydrosiloxane: 60 °C, H$_2$PtCl$_6$ (**1**), Karstedt's catalyst 60 °C (**2**), Pt/C at 100 °C (**3**).

Rajesh *et al.* [74] studied the materials obtained by the reaction of hydride and vinyl PDMS in the presence of Karstedt's catalyst using the solution casting method (Scheme 5). The process associated with the synthesis of a silicone rubber, featuring practically relevant properties, was studied by curing polymethylhydrosiloxane.
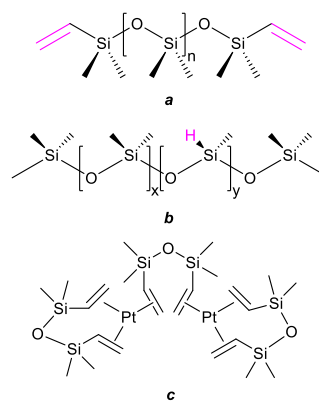
Scheme 5. Structures of vinyl-terminated PDMS (*a*), polymethylhydrogensiloxane (V-430) (*b*) where x and y are equal to 10, and Karstedt's catalyst (*c*).

All experiments in this work were performed with commercially available compounds: two vinyl-terminated PDMS liquid silicones U-10 and U-65, hydride cross-linking polymethylhydrogensiloxane (V-430), and a platinum catalyst (Karstedt's catalyst). The vinyl contents in U-10 and U-65 were 0.05 mmol/g and 0.03 mmol/g, and the polymer molar masses were 74400 and 85400, respectively. The cross-linking agent V-430 had the hydride content of 4.3 mmol/g.

The kinetic studies were carried out using IR spectroscopy, taking into account a decrease in the intensities of the νSi–H stretch at 2157 cm^{-1} and νC=C stretch at 1586 cm^{-1}. The reactions were carried out at three different temperatures, namely, 55 °C, 60 °C, and 75 °C using stoichiometric conditions, *i.e.* [Si–H]/[C=C] = 4.0, which was optimized based on the mechanical and cross-linking density measurements.

From the results obtained, it was found that the disappearance of both Si–H and C=C absorption bands corresponds to the first order kinetics. The complete curing was observed at a [hydride]/[vinyl] ratio of 4:1 for U-10, while the corresponding value for U-65 was 2:1. Hence, it was found that the theoretical stoichiometric ratio of 1:1 cannot always ensure complete curing. With the optimized ratio of both systems, significant improvement in the properties was observed compared to the conventional 1:1 ratio.

The kinetics of cross-linking was studied for the U-10 system under stoichiometric conditions, *i.e.* [Si–H]/[C=C] = 4.0. The measurements were carried out using FTIR spectroscopy at three different temperatures. The results appeared to correspond to a first order reaction relative to the transformation of both vinyl (C=C) and hydride (Si–H) groups (Fig. 11).
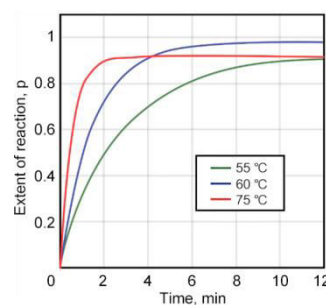

Figure 11. Transformation of Si–H groups over time at different temperatures during curing of U-10.

The kinetics of hydrosilylation was considered by Meister *et al.* [75] using several olefins as examples and Karstedt's catalyst as a platinum source. The kinetic measurements were carried out using NMR spectroscopy. The work included both mechanistic and kinetic studies of the reaction progress for the systems under investigation. It was shown that ^{195}Pt NMR spectroscopy could be a valuable tool for assessing the reactivity of the target substrate in hydrosilylation. In a typical experiment, Karstedt's catalyst and 10 equiv of the corresponding olefins (*i.e.* 5 equiv per Pt center) were diluted with toluene-d_8, followed by ^{195}Pt NMR studies at 293 and 333 K. The comparison of the resulting ^{195}Pt NMR spectra with that of neat Karstedt's catalyst allowed for evaluating the degree of conversion of divinyltetramethyldisiloxane (DVTMDS). The stepwise replacement of DVTMDS in Karstedt's catalyst can be described by two successive equilibria depicted in Scheme 6.
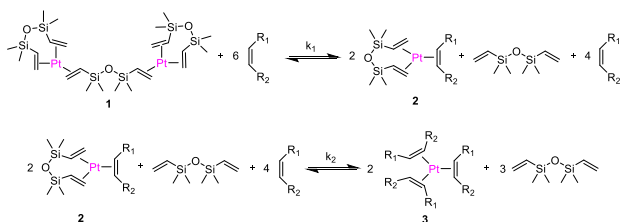
Scheme 6. Ligand exchange in Karstedt's catalyst under the action of the olefin substrates.

A kinetic study was performed using model substrates 1-octene and norbornene. The results of the experiments are presented in Figs. 12, 13.
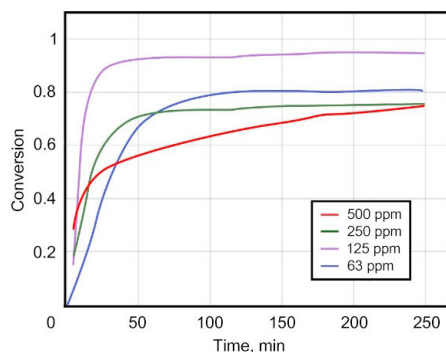

Figure 12. Hydrosilylation of 1-octene with HSiCl$_3$ at 313 K and different platinum concentrations [Pt].
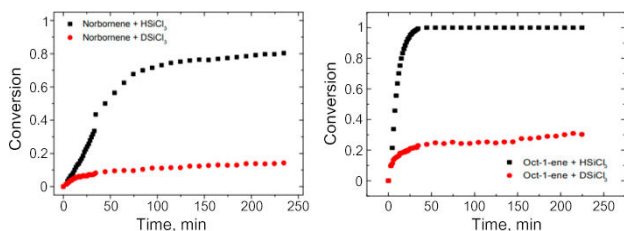

Figure 13. Results of the kinetic studies: hydrosilylation of norbornene with HSiCl$_3$ and DSiCl$_3$ at 333 K, Pt:norbornene:silane = 1:8000:16000, [norbornene] = 0.93 M in toluene-d_8 (left); hydrosilylation of 1-octene with HSiCl$_3$ and DSiCl$_3$ at 333 K, Pt:1-octene:silane = 1:8000:16000, [1-octene] = 0.93 M in toluene-d_8 (right).

It was demonstrated that the observed reaction orders can be best explained if considered in combination with the results of

the ^{195}Pt NMR spectroscopic and deuteration experiments. The coordination equilibria around the Pt center can be described as shown in Scheme 7.
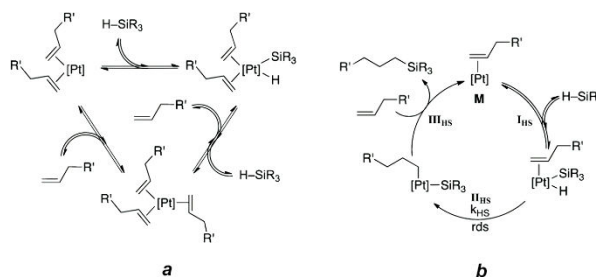
Scheme 7. Different types of platinum complexes depending on the coordination strength of the corresponding olefin (***a***); platinum-catalyzed hydrosilylation as determined by the deuteration experiments (***b***). Reprinted with permission from T. Meister *et al.*, *ACS Catal.*, **2016**, *6*, 1274–1284, DOI: 10.1021/acscatal.5b02624. Copyright (2016) American Chemical Society.

At very low olefin concentrations, the predominant form may be A, but typically Pt(0) is coordinated by three olefins (B). This species B is expected to be particularly stable if the corresponding olefin binds well to the platinum center. If the interaction is weak and the alkene is weakly bound, the oxidative addition by the H–SiR$_3$ bond with concomitant loss of one alkene ligand (formation of C) seems to be more likely.

As a result of the mechanistic studies presented above, the authors suggested the revised version of the Chalk–Harrod mechanism for platinum-catalyzed hydrosilylation (Scheme 8). The catalytic cycle includes the following steps: I$_{HS}$, oxidative addition of the hydrosilane; II$_{HS}$, migratory insertion of the olefin into the Pt–H bond; and III$_{HS}$, reductive elimination of the hydrosilylation product accompanied by the recoordination of the olefin. Depending on the olefin, II$_{HS}$ and III$_{HS}$ can compete with the III$_{IS}$–IV$_{IS}$ isomerization reaction or can be replaced by it to form the corresponding internal olefin rather than the hydrosilylation product, depending on the overall energy profile of the reaction. Based on the experimental data, it was concluded that the rate-limiting process in this reaction is not the reductive elimination of the hydrosilylation product, but the migratory insertion of the olefin. The nature of the active catalytic species M as well as the rate law of the hydrosilylation reaction are apparently related to the coordination strength of the olefin substrate.
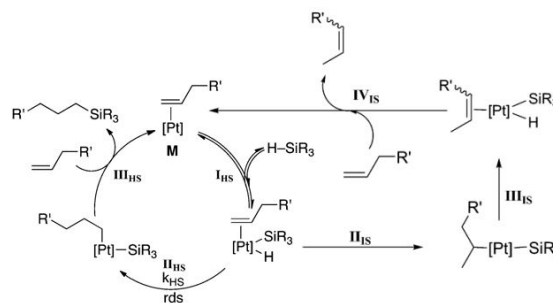

Scheme 8. Proposed revised mechanism for the platinum-catalyzed hydrosilylation using Karstedt's catalyst as a platinum source. Reprinted with permission from T. Meister *et al.*, *ACS Catal.*, **2016**, *6*, 1274–1284, DOI: 10.1021/acscatal.5b02624. Copyright (2016) American Chemical Society.

In summary, the combination of two deuterium-labeled experiments, [195]Pt NMR studies, and the in-depth kinetic investigations provides a basis for further development of the well-established Chalk–Harrod mechanism. It can be concluded that the coordination strength of the olefin plays a key role in the reaction kinetics. Furthermore, it is shown how various structural features of the active catalytic species can be inferred from the kinetic data.

Dietrich and Mejía [76] performed the synthesis of cyanopropyl-functionalized PDMS to determine the correlation between the conversion of Si–H groups and other parameters, such as the nature of reactants, catalyst, stoichiometry, and reaction temperature.

Four different copolymers (**1a–d**) were synthesized, changing the ratio between PDMS and PMHS (Table 2). For all reactions, the alkene/Si–H stoichiometry was equimolar. Compounds **1a–d** were synthesized using both homogeneous (Karstedt's catalyst) and heterogeneous (platinum on carbon, Pt@C) catalytic systems.

The kinetics of hydrosilylation with different siloxane starting materials and allyl cyanide were studied at temperatures from 60 to 80 °C using NMR spectroscopy. The reaction scheme is depicted in Scheme 9. The samples dissolved in a deuterated solvent were pre-cooled to stop the reaction.
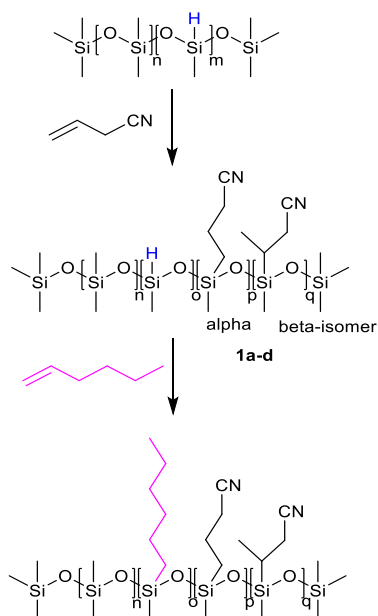
Scheme 9. Synthesis of copolymers **1a–d** by hydrosilylation with allyl cyanide and synthesis of copolymer **4** by hydrosilylation of 1-hexene.

Homogeneous Karstedt's catalyst and heterogeneous catalyst in the form of platinum on a carbon support were used as catalysts. It was noted that a decrease in the conversion of Si–H groups was observed in the series of polydimethylsiloxane copolymers **1a–d** (Table 2) with both homogeneous and heterogeneous catalysts, which correlates with a decrease in the amount of these functional groups in the starting material (Table 2). In addition, the conversions in series **1a–d** using the homogeneous (Karstedt's) catalyst were always significantly higher than those achieved with the heterogeneous system, even though the platinum loading was significantly higher in the latter case (5 times). This is most likely due to the lower content of active centers on the heterogeneous catalyst surface (compared to the homogeneous catalyst, where all Pt atoms are potentially active). According to the authors, the homogeneous catalytic system is preferable for this transformation.

Figure 14 shows the dependences of the concentration of Si–H groups (inverse) on time from **1b** to **1d**. The authors emphasized that in all cases the kinetic curves show two different modes of consumption of Si–H groups over time, which is demonstrated by the bends. This change in the reaction rate depends on the starting material, as well as on the reaction temperature. Based on this, it was concluded that the partial deactivation of the catalyst occurs after a rapid initial stage, referring to Müller *et al.* [77]. Furthermore, the formation of metal clusters and aggregates at later stages of hydrosilylation for Karstedt's catalyst is well described in the literature [78]. Although, as the authors of the article noted, the biphasic kinetic mode has not been fully described.
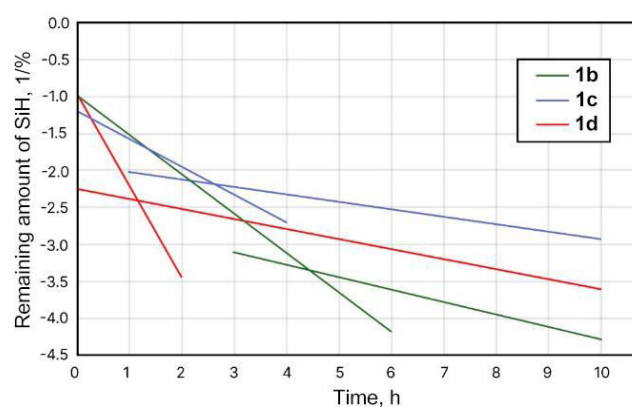
Figure 14. Dependence of the conversion of Si–H groups on the starting materials of polymeric hydridomethylsiloxane and time in the hydrosilylation reaction with allyl cyanide at 80 °C (**1b,d**).

For comparison, the kinetic parameters of hydrosilylation with a non-polymer starting material, namely, D^H_4 cyclosiloxanes were also determined (Fig. 15). There are no bends on the curves, and the reaction rates are constant, which indicates that the reduced conversion depends not only on the nature of the cyano group and the distribution of D units in siloxanes, as was assumed earlier, but also on the properties of the starting material.
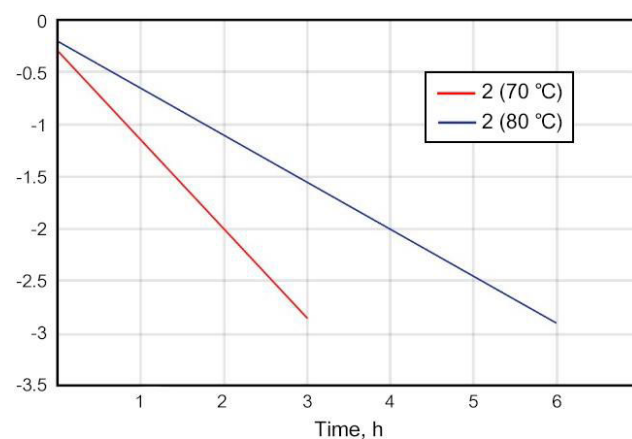

Figure 15. Dependence of the conversion of Si–H groups on the initial monomeric cyclosiloxane materials and time in the hydrosilylation reaction with allyl cyanide.

Table 2. Synthesis of copolymers **1a–d** using homogeneous (Karstedt's catalyst, 0.1 mol % Pt) and heterogeneous (Pt@C, 0.5 mol % Pt) platinum catalysts. The conversions were calculated based on the ^{1}H NMR spectroscopic data

Entry	Product	Si–H molar content [%]	Catalyst	Conversion	Yield α-isomer	Yield β-isomer	MW[g/mol]
1	**1a**	100	Karstedt's cat.	90	11.9	1	2985
2			Pt@C	56	13.0	1	4190
3	**1b**	50	Karstedt's cat.	83	8.2	1	3441
4			Pt@C	56	8.3	1	3337
5	**1c**	25	Karstedt's cat.	72	8.0	1	4371
6			Pt@C	25	24	1	4292
7	**1d**	15	Karstedt's cat.	55	6.9	1	3760
8			Pt@C	22	10.0	1	4351

The work showed a good correlation between the conversion of Si–H groups and other parameters, such as the nature of reagents, catalyst deactivation, and reaction energy. In addition, the kinetic studies demonstrated that both the reaction order and activation energy strongly depend on the nature of reagents.

The investigations on the kinetics of hydrosilylation are still relevant today. Thus, recently Jalkanen [79] studied the kinetics of such reactions using differential scanning calorimetry and rheometry and applied Vyazovkin's advanced isoconversional method [80] to calculate the kinetic data of reactions.

In the mentioned work, commercially available silicone rubbers MED4-4516 (cured with peroxide) and MED-4735 (cured with platinum) were used as model compounds for the kinetic measurements. The measurements were carried out using differential scanning calorimetry. All experiments began with a 5-min isothermal curing at 25 °C. The samples were heated at four different heating rates, namely 5, 10, 15, and 20 deg/min. The samples were heated to 200 °C for the first three heating rates and to 220 °C at a heating rate of 20 deg/min. All measurements were conducted under a constant nitrogen flow. The results of DSC studies are presented in Fig. 16.
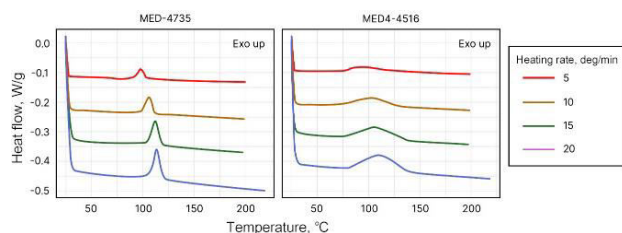
Figure 16. DSC curves for two different silicone rubbers measured at four different heating rates.

Using the results obtained by the DSC method and further processing of the data by the following formula

$$\alpha = \frac{\int_{t0}^{t} \left(\frac{dH}{dt}\right) dt}{\int_{t0}^{tf} \left(\frac{dH}{dt}\right) dt} = \frac{\Delta H}{\Delta H_{tot}},$$

the kinetic curves of cross-linking reactions at different temperatures can be obtained, which are presented in Fig. 17. In addition, it is possible to determine the activation energy values from the data presented in Fig. 18. The shapes of the resulting curves clearly differ for the platinum and peroxide curing systems. The peroxide curing system exhibits a higher overall activation energy with a higher activation energy barrier at the reaction beginning.
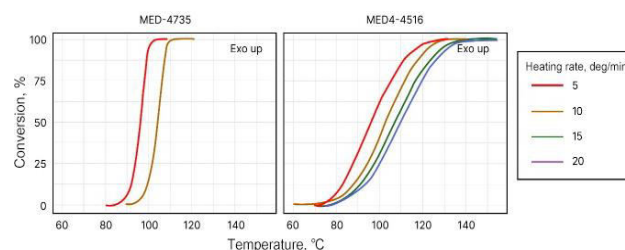
Figure 17. Conversion curves calculated from the DSC data for both silicone rubbers showing the development of the cross-linking reaction at different heating rates.
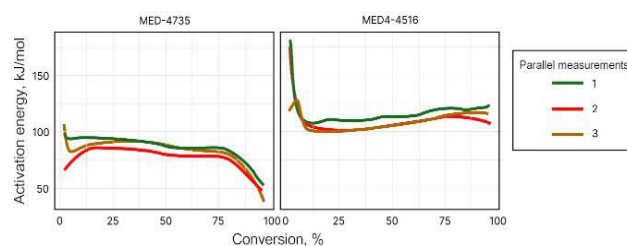
Figure 18. Activation energies of the reactions depending on the conversion degree.

Figure 19 compares the experimentally measured reaction rates and those calculated by Vyazovkin's method: some discrepancies can be noted, which are more marked in the experiments at 100 °C.
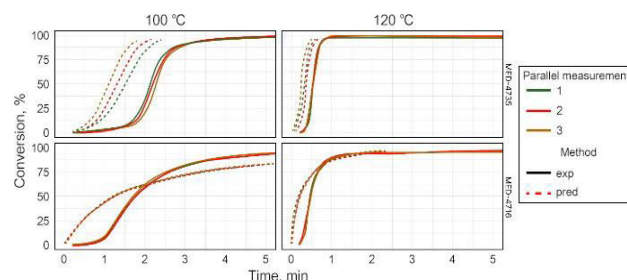
Figure 19. Comparison of the experimental (solid lines) and predicted (dashed lines) cross-linking rates of epy silicone rubber catalyzed by platinum and peroxide.

The authors explained this divergence by the fact that the sample needs some time to reach the specified temperature, which leads to an experimental lag from the theoretically ideal situation. It is also evident that the error is not so significant for temperatures that significantly exceed the minimum required curing temperature.

In summary, it can be stated that Vyazovkin's method is effective in predicting the cross-linking behavior of platinum and peroxide curing of silicones. The kinetic predictions obtained by the isoconversional method show good correlation with the experimental results, despite the necessity of introduction of corrections into the calculations. The results obtained demonstrate the importance of measurements immediately after mixing the materials.

Pan *et al.* [81] developed a new platinum-based catalyst (COP1-T-Pt), which is comparable in the efficiency to natural enzymes (Scheme 10). This selective platinum catalyst is believed to be highly active for industrially significant hydrosilylation processes and for a wide range of substrates when a porous cage ligand (the ligand is used to localize the platinum catalyst around the catalytically active site) is used to retain the catalytically active center. This biomimetic catalyst exhibits good selectivity due to the cage confinement effect, which amplifies small steric differences in the abrupt changes in reactivity for similar functional groups in the molecule.
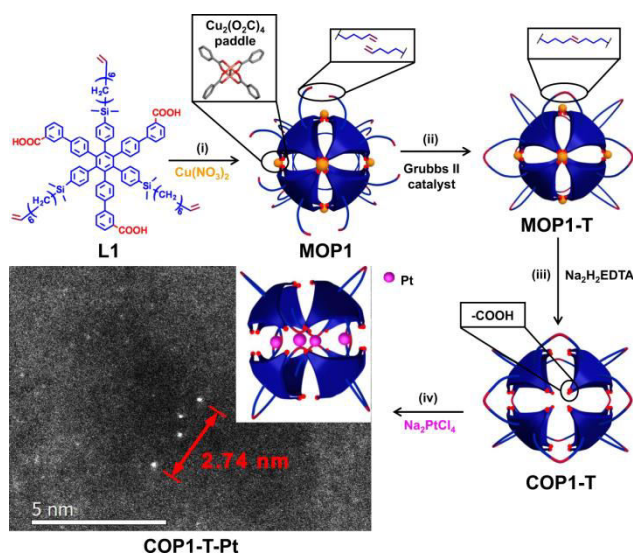
Scheme 10. Synthesis of COP1-T-Pt: (i) Cu(NO$_3$)$_2$, DMF, 60 °C, 24 h, 95% yield; (ii) 1 mol % of Grubbs' catalyst II, THF, 90% yield; (iii) Na$_2$H$_2$EDTA, THF, H$_2$O, 99% yield; (iv) 4 equiv. of Na$_2$PtCl$_4$ in THF followed by the reduction with 100 equiv. of dimethylphenylsilane. Reprinted with permission from G. Pan *et al.*, *Nat. Commun.*, **2021**, *12*, 64, DOI: 10.1038/s41467-020-20233-w.

The kinetic curve of the reaction of triethoxysilane with hexene in the presence of the above-mentioned catalyst is shown in Fig. 20, apparently obtained from ^{1}H DOSY data. COP1-T-Pt demonstrated high catalytic efficiency in the hydrosilylation reaction between triethoxysilane and 1-hexene with a record high TOF of 78000 h^{-1} compared to conventional Karstedt's catalyst (6400 h^{-1}) (about 12 times) and an activation energy of about 40 kJ/mol. In addition, the authors claimed that the kinetic study of this process catalyzed by COP1-T-Pt revealed the behavior according to the Michaelis–Menten model [82, 83], which has never been reported for the hydrosilylation reaction catalyzed by Pt catalysts. However, a detailed description of the procedure for establishing the TOF value by this method is missing in the work, although it is of considerable interest, especially in the case of practical application of the new catalyst.
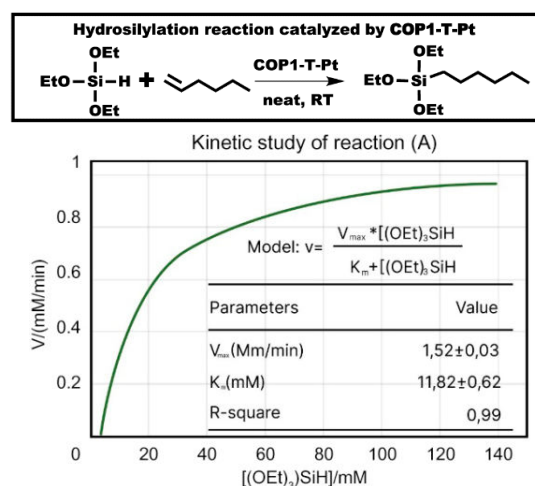

Figure 20. COP1-T-Pt-catalyzed hydrosilylation reaction between triethoxysilane and 1-hexene and the kinetic study in neat 1-hexene at room temperature and the catalyst concentration of 1.67·10^{-6} M. Reprinted with permission from G. Pan *et al.*, *Nat. Commun.*, **2021**, *12*, 64, DOI: 10.1038/s41467-020-20233-w.

The initial reaction rate was measured at a 1-hexene conversion of less than 2%. The error bar represents the standard error for each initial reaction rate calculated using ten points. The selectivity for triethoxysilane, which is a large-scale product and is used as a precursor in many industries, was also evaluated (Scheme 11).
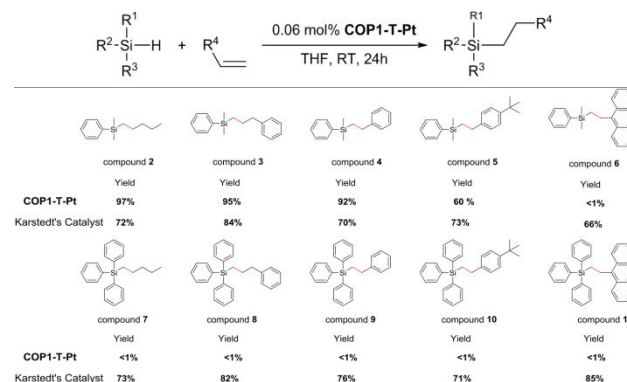
Scheme 11. Hydrosilylation of trialkoxysilanes with different substrates demonstrating the site-selective effect for COP1-T-Pt. Yields (by GC-MS) are based on moles of reactants with smaller amounts. Reprinted with permission from G. Pan *et al.*, *Nat. Commun.*, **2021**, *12*, 64, DOI: 10.1038/s41467-020-20233-w.

As a result of the studies, the cage Pt catalyst demonstrated very high catalytic activity in the industrially important hydrosilylation reaction. It was shown that this catalyst is ten times more active than classical Karstedt's catalyst and is also suitable for recycling. This catalyst not only demonstrated tolerance to a wide range of substrates, but also showed size-selective catalysis and provided catalysis for substrates with several functional groups, which, according to the authors, opens up the way to industrially produced alkoxysilanes. Unfortunately, the authors did not consider the issues of economic efficiency of this catalyst, but the possibilities of reuse and high activity of the catalyst may compensate for its likely high cost.

4. Study of the kinetics of the hydrosilylation reaction with miscellaneous catalysts based on other metals

The hydrosilylation reaction does not necessarily require the use of platinum-based catalysts. A literature survey revealed the increasing number of examples of the use of other catalytic systems, such as compounds of zinc [84], rhodium [85], iridium [86], iron [87–89], cobalt [90], magnesium [91], manganese [92], palladium [99], *etc*. However, the kinetics of such reactions have been studied in only a few works.

Pérez *et al.* [93] demonstrated how a rhenium complex catalyzes the hydrosilylation of benzaldehyde (Scheme 12). The reactions were carried out at different temperatures, catalyst concentrations, and with different silane reagents in acetonitrile or under neat conditions.

(1a) R = C_6F_5
(1b) R = Mes

(2a) R = C_6F_5, X = OTf; (2b) R = Mes, X = OTf
(3a) R = C_6F_5, X = BArF$_4$; (3b) R = Mes, X = BArF$_4$
(4a) R = C_6F_5, X = BF$_4$; (4b) R = Mes, X = BF$_4$
(5a) R = C_6F_5, X = PF$_6$; (5b) R = Mes, X = PF$_6$
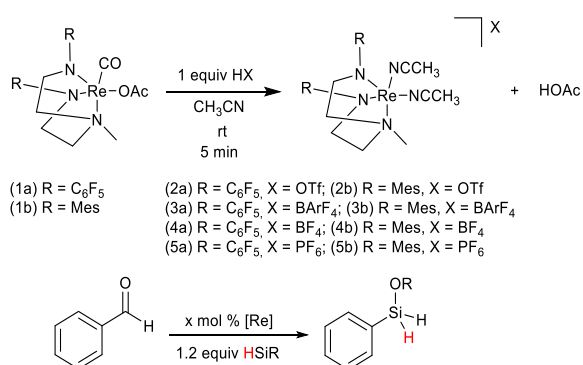
Scheme 12. Synthesis of the rhenium complex and catalytic hydrosilylation of benzaldehyde.

The kinetic studies were performed using ^{1}H NMR spectroscopic data to determine the dependences for each reactant, during which a time profile under pseudo-first order conditions was observed (Fig. 21). The results suggest a general first-order rate law (Fig. 21, left). A first-order dependence according to Ref. [4a] (Fig. 21) was also obtained by plotting the observed rate constants (K_{obs}) against the rhenium concentration (Fig. 21, right).
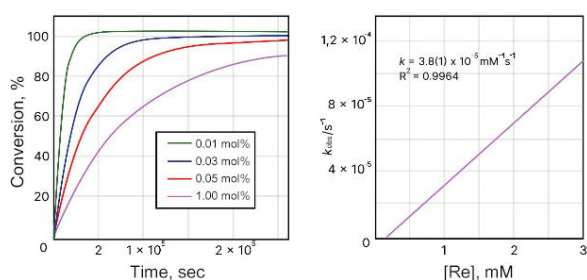

Figure 21. Time profiles of the catalytic hydrosilylation of benzaldehyde with 4a (left). Reaction conditions: [benzaldehyde] = 2.77 M; [HSiMe$_2$Ph] = 3.324 M; [2-bromomesitylene] = 1.385 M; [4a] = 0.0279 mmol (0.01 mol %), 0.829 mmol (0.03 mol%), 1.385 mmol (0.5 mol%), or 2.77 (1 mol%).

The order relative to benzaldehyde was determined by performing the kinetic experiments in neat HSiMe$_2$Ph. The decomposition of benzaldehyde was monitored by GC using 2-bromomesitylene as an internal standard (Fig. 22). Given that

the overall reaction features the first order, the zero-order dependence on [benzaldehyde] suggests that the reaction features the first order relative to the silane.
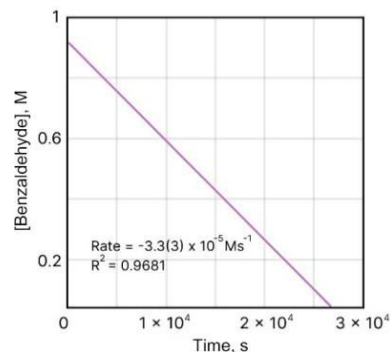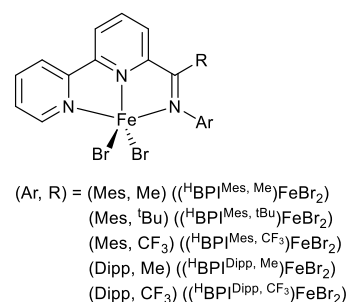

Figure 22. Kinetic plot of [benzaldehyde] *vs.* time. Reaction conditions: [4a] = 0.921 mM; [Benzaldehyde] = 0.921 M; [HSiMe$_2$Ph] = 5.48 M. The concentration of benzaldehyde was determined by GC by integrating the benzaldehyde peak against the internal standard 2-bromomesitylene (0.438 M).

Based on the kinetic experiments, the following rate equation for the hydrosilylation of benzaldehyde catalyzed by compound 4a was suggested

$$\frac{d[PhCH_2OSiMe_2Ph]}{dt} = k[4a][HSiMe_2Ph].$$

Thus, the authors showed in their work that the cationic rhenium(III) complexes of DAAm are highly effective catalysts for the hydrosilylation of aldehydes. The kinetic data showed that the reaction rate features the first order relative to [silane] and [4a] and does not depend on the aldehyde concentration. However, the transition from ^{1}H NMR to GC in the case of measuring in neat HSiMe$_2$Ph seems to be strange. Moreover, the authors did not explain the necessity of this transition.

Toya *et al.* [88] obtained ketimine-type iminobipyridine iron complexes (Scheme 13). These complexes appeared to be effective catalysts for the hydrosilylation of olefins with primary, secondary and tertiary silanes.

(Ar, R) = (Mes, Me) ((HBPIMes, Me)FeBr$_2$)
(Mes, tBu) ((HBPIMes, tBu)FeBr$_2$)
(Mes, CF$_3$) ((HBPIMes, CF$_3$)FeBr$_2$)
(Dipp, Me) ((HBPIDipp, Me)FeBr$_2$)
(Dipp, CF$_3$) ((HBPIDipp, CF$_3$)FeBr$_2$)

Scheme 13. Ketimine-type iminobipyridine iron complexes. Reprinted with permission from Y. Toya *et al.*, *Organometallics*, **2017**, *36*, 1727–1735, DOI: 10.1021/acs.organomet.7b00087. Copyright (2017) American Chemical Society.

The reaction kinetics were analyzed by HPLC to determine the yield of the hydrosilylated product(s). In order to compare the catalytic activity of the resulting iminobipyridine iron complexes with that of Karstedt's catalyst, the hydrosilylation reaction catalyzed by Karstedt's catalyst was also investigated under the same conditions. The results are shown in Scheme 14.

$$\text{silane} \ + \ 2\ \text{eq} \ \ \text{1-octene} \ \xrightarrow[\text{r.t., 24 h}]{\substack{\text{Fe complex cat.} \\ \text{NaBHEt}_3\ \text{cat.}}} \ \text{hydrosilylated product}$$
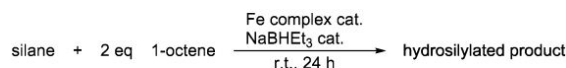
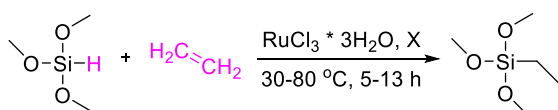| entry	Fe complex	amt of Fe complex (mol %)[b]	silane	product (yield (%), TON)[c]		total TON[d]
1	(^{H}BPI^{Mes,H})FeBr$_2$	0.01	PhSiH$_3$	Ph(octyl)SiH$_2$ (21, 2140)	Ph(octyl)$_2$SiH (1, 80)	2300
2	(^{H}BPI^{Mes,Me})FeBr$_2$			Ph(octyl)SiH$_2$ (56, 5610)	Ph(octyl)$_2$SiH (26, 2640)	10890
3	(^{H}BPI^{Mes,tBu})FeBr$_2$			Ph(octyl)SiH$_2$ (15, 1480)	Ph(octyl)$_2$SiH (1, 80)	1640
4	(^{H}BPI^{Mes,CF3})FeBr$_2$			Ph(octyl)SiH$_2$ (67, 6660)	Ph(octyl)$_2$SiH (29, 2850)	12360
5	(^{H}BPI^{Dipp,H})FeBr$_2$			Ph(octyl)SiH$_2$ (65, 6460)	Ph(octyl)$_2$SiH (31, 3110)	12680
6	(^{H}BPI^{Dipp,Me})FeBr$_2$			Ph(octyl)SiH$_2$ (60, 5950)	Ph(octyl)$_2$SiH (8, 750)	7450
7	(^{H}BPI^{Dipp,CF3})FeBr$_2$			Ph(octyl)SiH$_2$ (63, 6330)	Ph(octyl)$_2$SiH (7, 680)	7690
8	Karstedt's catalyst			Ph(octyl)SiH$_2$ (3, 260)	Ph(octyl)$_2$SiH (0, 0)	260
9	(^{H}BPI^{Mes,H})FeBr$_2$	0.01	Ph$_2$SiH$_2$	Ph$_2$(octyl)SiH (65, 6480)	Ph$_2$(octyl)$_2$Si (0, 0)	6480
10	(^{H}BPI^{Mes,Me})FeBr$_2$			Ph$_2$(octyl)SiH (31, 3120)	Ph$_2$(octyl)$_2$Si (65, 6460)	16040
11	(^{H}BPI^{Mes,tBu})FeBr$_2$			Ph$_2$(octyl)SiH (42, 4190)	Ph$_2$(octyl)$_2$Si (0, 0)	4190
12	(^{H}BPI^{Mes,CF3})FeBr$_2$			Ph$_2$(octyl)SiH (54, 5370)	Ph$_2$(octyl)$_2$Si (45, 4490)	14350
13	(^{H}BPI^{Dipp,H})FeBr$_2$			Ph$_2$(octyl)SiH (94, 9380)	Ph$_2$(octyl)$_2$Si (1, 70)	9520
14	(^{H}BPI^{Dipp,Me})FeBr$_2$			Ph$_2$(octyl)SiH (71, 7100)	Ph$_2$(octyl)$_2$Si (7, 710)	8520
15	(^{H}BPI^{Dipp,CF3})FeBr$_2$			Ph$_2$(octyl)SiH (75, 7530)	Ph$_2$(octyl)$_2$Si (1, 110)	7750
16	Karstedt's catalyst			Ph$_2$(octyl)SiH (92, 9210)	Ph$_2$(octyl)$_2$Si (0, 0)	9210
17	(^{H}BPI^{Mes,H})FeBr$_2$	0.1	Ph$_2$MeSiH	Ph$_2$Me(octyl)Si (74, 741)		741
18	(^{H}BPI^{Mes,Me})FeBr$_2$			Ph$_2$Me(octyl)Si (80, 795)		795
19	(^{H}BPI^{Mes,tBu})FeBr$_2$			Ph$_2$Me(octyl)Si (13, 132)		132
20	(^{H}BPI^{Mes,CF3})FeBr$_2$			Ph$_2$Me(octyl)Si (65, 645)		645
21	(^{H}BPI^{Dipp,H})FeBr$_2$			Ph$_2$Me(octyl)Si (49, 494)		494
22	(^{H}BPI^{Dipp,Me})FeBr$_2$			Ph$_2$Me(octyl)Si (62, 621)		621
23	(^{H}BPI^{Dipp,CF3})FeBr$_2$			Ph$_2$Me(octyl)Si (1, 7)		7
24	Karstedt's catalyst			Ph$_2$Me(octyl)Si (93, 928)		928

Scheme 14. Reaction conditions: room temperature, 24 h, Schlenk tube, [silane]:[1-octene] = 1:2, [Fe complex]:[NaBHEt$_3$] = 1:20. [b] mol % = [Fe complex]/[silane] × 100; [c] determined by HPLC. The values are based on the initial concentration of a hydrosilane. Reprinted with permission from Y. Toya *et al.*, *Organometallics*, **2017**, *36*, 1727–1735, DOI: 10.1021/acs.organomet.7b00087. Copyright (2017) American Chemical Society.

In all cases, the selective anti-Markovnikov addition occurred and only 1-octyl-substituted silanes were formed; 2-octyl-substituted silanes or any other isomers were not detected.

In addition, the authors studied the effect of substituents on the catalytic activity. The control over the rate of each reaction is important for the selective formation of given alkylated silanes and can be achieved by changing the amount of the catalyst. It is assumed that the alkylation of silanes by hydrosilylation of olefins occurs in a stepwise manner: first, a monoalkylated product is formed, then a dialkylated product is formed, which was also detected in Ref. [94] where the process of hydrolsilylation of a carbosilane dendrimer with an allyl shell with didodecyl(methyl)silane in an amount necessary to replace 50% of allyl groups of the outer layer of the dendrimer was shown. In this work, the selectivity of the substitution of every second allyl group at the silicon atom was observed due to the sequential introduction of functional groups into the reaction.

Liu *et al.* [95] described an efficient one-step synthesis of ethyltrimethoxysilane (ETMS) from trimethoxysilane and ethylene, catalyzed by ruthenium chloride hydrate (RuCl$_3$·3H$_2$O–H$_2$O) and promoted by water or alcohols (Scheme 15).

The authors studied the effect of the catalyst content on the yield of ETMS at a constant molar ratio of H$_2$O to RuCl$_3$·3H$_2$O and other conditions. The results are presented in Fig. 23.
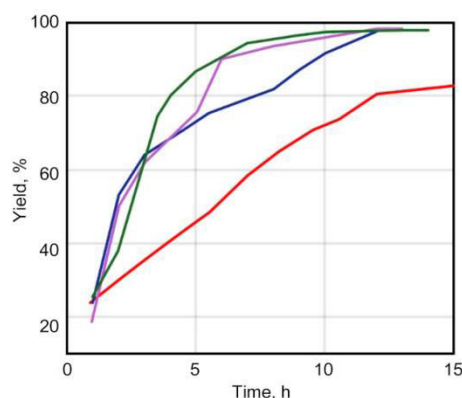
Figure 23. Effect of the catalyst content and promoter/catalyst molar ratio on the yield of ETMS. Catalyst content: $1.1\cdot10^{-4}$ (blue line), $1.1\cdot10^{-4}$ (green line), $3.3\cdot10^{-5}$ (red line), $3.3\cdot10^{-5}$ (purple line). Molar ratio of H$_2$O to ruthenium: 3.5:1 (blue line), 8.4:1 (green line), 3.5:1 (red line), 33.6:1 (purple line). The indicated catalyst concentration represented the molar ratio of ruthenium to trimethoxysilane.

It can be concluded that, under conditions of a relatively high catalyst concentration, the amount of water does not have a noticeable effect on the yield of the target product. However, at the low catalyst concentrations, the amount of water has a significant effect on the yield of ETMS.

Scheme 15. Synthesis of ethyltrimethoxysilane by hydrogenation catalyzed by Ru.

The effect of temperature on the hydrosilylation reaction was also studied. For this purpose, five reactions were carried out at temperatures from 30 to 80 °C. The results are shown in Fig. 24. When the reaction was carried out at 30 °C, its rate was very low, and the yield of ETMS did not exceed 25% after 5 h. With an increase in the reaction temperature, the reaction rate increased rapidly, and when the reaction was carried out at 40 °C for 5 h, a yield of 93% could be obtained. However, as the temperature continued to increase, the yield of ETMS gradually decreased. The authors explained this phenomenon by the fact that at elevated temperatures, TMS is capable of converting into TEOS. Thus, the optimal temperature range for the reaction of ethylene hydrosilylation with trimethoxysilane was 40–60 °C, since in this interval the reaction can proceed rapidly and, at the same time, the degree of disproportionation of trimethoxysilane is insignificant.
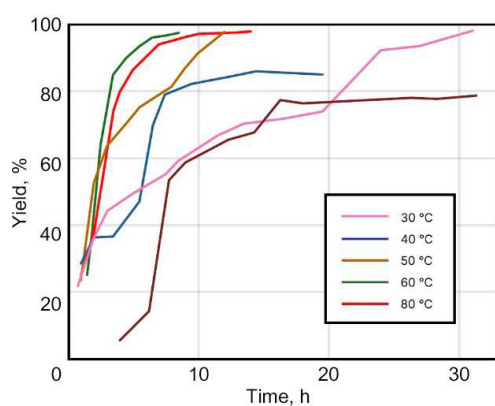

Figure 24. Effect of the reaction temperature on the yield of ETMS. The concentration of ruthenium was $9.4 \cdot 10^{-6}$ mol per mole of trimethoxysilane; the molar ratio of H_2O to $RuCl_3 \cdot 3H_2O$ was 110.7 for each reaction.

In addition, various factors affecting the selectivity and yield of the target product were considered in the study. It was found that the yield of ethyltrimethoxysilane was significantly affected by the concentration of ruthenium chloride hydrate, the molar ratio between water and ruthenium chloride hydrate, and the reaction temperature. The kinetic studies and the structure of each component in the hydrosilylation product were qualitatively characterized by GC-MS. The applicability of this method for the investigation of kinetics has already been discussed above.

Chang *et al.* [96] reported the synthesis of a nickel-based catalyst ((NHC)Ni(0) complex (NHC = *N*-heterocyclic carbene)) and its compatibility with various systems for hydrosilylation.

During the investigations, it was found that the catalyst demonstrated good compatibility with a wide range of substrates (Scheme 16); in particular, it tolerates sensitive functional groups and heteroaromatic compounds. Hexane was used as a solvent in the reaction instead of toluene to facilitate purification of the product. Chlorosilanes have not often been studied in hydrosilylation reactions, and it was shown earlier that nickel-based catalysts allow for replacing Si–Cl bonds for Si–H bonds, with the reduced products often being the main ones, so the involvement of chlorosilanes in the list of substrates is a significant achievement, especially in view of their importance for polysiloxane chemistry.
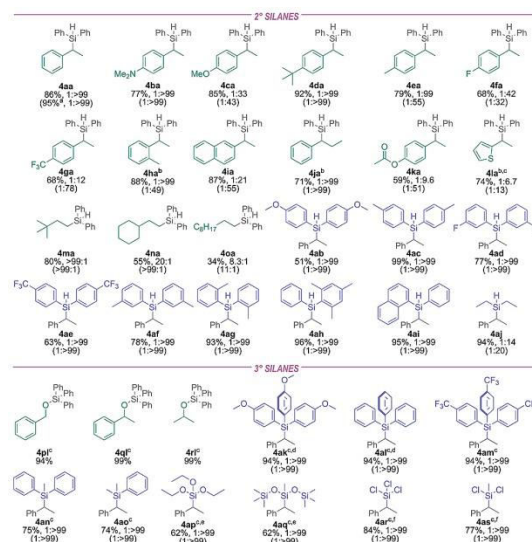
Scheme 16. Yields of individual compounds and selectivity (l/b) determined from the relative ^{1}H NMR integrations. Reprinted with permission from A. S.-m. Chang *et al.*, *ACS Catal.*, **2022**, *12*, 11002–11014, DOI: 10.1021/acscatal.2c03580. Copyright (2022) American Chemical Society.

The kinetic measurements in the considered work were carried out using ^{1}H NMR spectroscopy (Fig. 25) in deuterotoluene at 75 °C. Figure 26 shows the kinetic curve of one of the compounds obtained (4aa). The order of each of the reactants, namely, styrene, diphenylsilane, and catalyst 1e was obtained by measuring the initial reaction rates at different concentrations of the reactant or catalyst. The authors measured the rate of formation of product 4aa as a function of the catalyst concentration (2.19–21.9 mM). Under standard reaction conditions, the rates were too high to obtain the initial reaction rates; therefore, the reaction temperature was reduced to 80 °C. The catalyzed hydrosilylation of compounds 2a and 3a (shown in Fig. 25) was dependent on the [Ni] half-order (0.6 ± 0.1). This value is consistent with the previously reported monomeric catalysts that are activated by pre-equilibrium ligand dissociation.
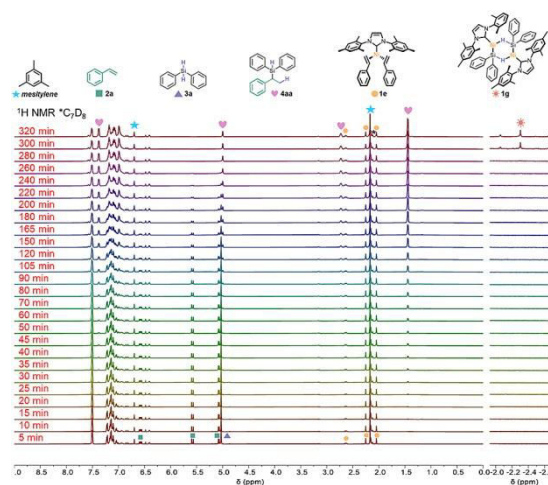

Figure 25. ^{1}H NMR monitoring of the reaction of styrene and diphenylsilane catalyzed by 1e. Reprinted with permission from A. S.-m. Chang *et al.*, *ACS Catal.*, **2022**, *12*, 11002–11014, DOI: 10.1021/acscatal.2c03580. Copyright (2022) American Chemical Society.

Figure 26. Kinetic profile of [4aa] (mM) *vs.* time. Reprinted with permission from A. S.-m. Chang *et al*., *ACS Catal*., **2022**, *12*, 11002–11014, DOI: 10.1021/acscatal.2c03580. Copyright (2022) American Chemical Society.
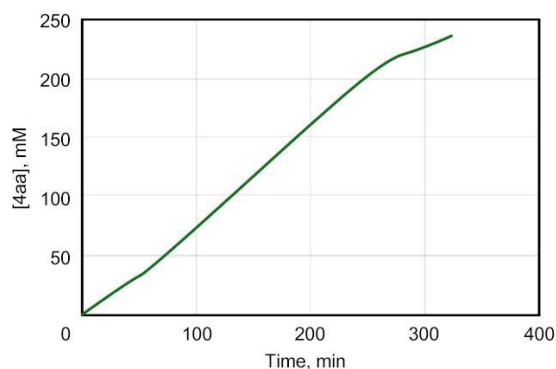
The data presented in this work show that the range of silanes and alkenes that undergo hydrosilylation demonstrate the broad applicability of (NHC)-Ni(0) catalytic system. The authors also demonstrated that the steric bulk of NHC can be tuned to enhance the yield of particularly unreactive silanes.

In summary, this report demonstrated that nickel complexes are active in the selective hydrosilylation of alkenes with secondary or tertiary silanes, including industrially important alkoxy and chlorosilanes. The range of alkenes and silanes that can be introduced into the reaction owing to catalysis by Ni compounds was also expanded. The experiments were conducted to study the kinetics of reactions as well as mechanistic aspects. The experiments using deuterium labels showed that the hydrosilylation occurs by the Chalk–Harrod mechanism, with the alkene being reversibly inserted into the Ni–H bond.

Conclusions

The variety of conditions for hydrosilylation, namely, the possibility of using a homogeneous or heterogeneous catalyst as well as a catalyst in a separate phase, different solvents or their absence certainly has a strong effect on the kinetics. Particular attention should be drawn to the necessity of understanding the homogeneity or heterogeneity of the catalyst, the processes of leaching of active species [97, 98]. Furthermore, significant factors that are likely to determine the rate of the hydrosilylation reaction are the type and spatial arrangement of the reacting functional groups participating in the reaction, as well as additional factors such as reaction components or functional groups that do not participate in the reaction but are capable of coordinating with platinum and other components of the reaction medium. Nevertheless, each of these processes can be adequately classified in order to select appropriate methods for studying the catalyst effectiveness and compiling kinetic equations. Only such a complex approach can help to outline clear relationships of the hydrosilylation reaction.

Summarizing the literature data, it can be concluded that, despite the widespread use of hydrosilylation in science and industry, insufficient attention is paid to the investigations on the kinetic features of this process. This looks especially strange given the ample opportunities of different physicochemical methods for analyzing both the reaction mixture and reaction products, which are applicable to the study of the kinetics of the hydrosilylation reaction. However, it is important to note that the kinetic studies of hydrosilylation processes are becoming increasingly important, since the search for new catalytic systems is gaining popularity, and the kinetics of the processes is important both for establishing or confirming the mechanism and for comparing the efficiency of catalysts.

It is noteworthy that there are a significant number of reports in which the kinetic features of the hydrosilylation reaction is studied by gas chromatography and are exposed to uncontrolled temperature impact, which casts doubt on the reliability of the resulting kinetic parameters.

From the literature survey it is clear that the most effective tools for studying kinetics are NMR spectroscopic methods, a wide variety of which allows for extracting diverse information not only on the conversion of functional groups, but also on the type of addition, side processes, *etc*. The unique approaches include freezing the reaction mixture at various stages of the process and analyzing the state of platinum. The only disappointment is that the selection of points for analysis was carried out using the above-mentioned GC methods, which considerably reduces the significance of the resulting data, but the main conclusions about monoplatinum active centers remain relevant. It remains only to regret that this technique was not applied at the final stages of the process.

Despite the abundance of new platinum and non-platinum catalytic systems, their comparison has not yet been brought to a common denominator. Apparently, it is time to create a kind of test template for minimal unification of the process of comparing the catalyst efficiency. Thus, despite the existence of several known model systems, it is necessary to introduce several additional criteria, such as versatility (the ability to catalyze both monomeric and polymeric transformations); it is necessary to define the majority of existing catalytic systems as evolving. During the reaction, a catalyst converts to some intermediate state which, in fact, promotes the process. In addition, it is also necessary to take into account the number of single acts per mole of a catalyst.

All this makes the study of the kinetics of the hydrosilylation reaction increasingly relevant and necessary for its understanding and application in the chemical industry.

Acknowledgements

Corresponding author

* E-mail: krylov@ispm.ru (F. D. Krylov).

References

1. V. Chandrasekhar, *Inorganic and Organometallic Polymers*, Springer, Berlin, Heidelberg, **2005**. DOI: 10.1007/b137079

2. *Silicon-Containing Polymers. The Science and Technology of Their Synthesis and Applications*, R. G. Jones, W. Ando, J. Chojnowsky (Eds.), Springer, Dordrecht, **2000**. DOI: 10.1007/978-94-011-3939-7

3. M. A. Brook, *Silicon in Organic, Organometallic, and Polymer Chemistry*, Wiley, New York, **2000**.

4. *Silicon Containing Hybrid Copolymers*, C. He, Z. Li (Eds.), Wiley, Weinheim, **2020**.

5. *Silicon Based Polymers. Advances in Synthesis and Supramolecular Organization*, F. Ganachaud, S. Boileau, B. Boury (Eds.), Springer, Dordrecht, **2008**. DOI: 10.1007/978-1-4020-8528-4

6. J. C. McDonald, G. M. Whitesides, *Acc. Chem. Res.*, **2002**, *35*, 491–499. DOI: 10.1021/ar010110q

7. E. Berthier, E. W. K. Young, D. Beebe, *Lab Chip*, **2012**, *12*, 1224–1237. DOI: 10.1039/C2LC20982A

8. T. Köhler, A. Gutacker, E. Mejiá, *Org. Chem. Front.*, **2020**, *7*, 4108–4120. DOI: 10.1039/d0qo01075h

9. M. G. Mohammed, R. Kramer, *Adv. Mater.*, **2017**, *29*, 1604965. DOI: 10.1002/adma.201604965

10. P. Mazurek, M. A. Brook, A. L. Skov, *Langmuir*, **2018**, *34*, 11559–11566. DOI: 10.1021/acs.langmuir.8b02039

11. C. T. K. Khoo, *J Hand Surg.: Br. Eur. Vol.*, **1993**, *18*, 679–686. DOI: 10.1016/0266-7681(93)90222-2

12. P. Hu, Q. Xie, C. Ma, G. Zhang, *Langmuir*, **2020**, *36*, 2170–2183. DOI: 10.1021/acs.langmuir.9b03926

13. Y. Zhuo, S. Xiao, A. Amirfazli, J. He, Z. Zhang, *Chem. Eng. J.*, **2021**, *405*, 127088. DOI: 10.1016/j.cej.2020.127088

14. E. Yilgör, I. Yilgör, *Prog. Polym. Sci.*, **2014**, *39*, 1165–1195. DOI: 10.1016/j.progpolymsci.2013.11.003

15. S. B. Campbell, Q. Wu, J. Yazbeck, C. Liu, S. Okhovatian, M. Radisic, *ACS Biomater. Sci. Eng.*, **2021**, *7*, 2880–2899. DOI: 10.1021/acsbiomaterials.0c00640

16. *Hydrosilylation. A Comprehensive Review on Recent Advances*, B. Marciniec (Ed.), *Adv. Silicon Sci.*, vol. 1, Springer, Dordrecht, **2009**. DOI: 10.1007/978-1-4020-8172-9

17. K. A. Bezlepkina, S. A. Milenin, N. G. Vasilenko, A. M. Muzafarov, *Polymers*, **2022**, *14*, 2408. DOI: 10.3390/polym14122408

18. Y. Abe, T. Gunji, *Prog. Polym. Sci.*, **2004**, *29*, 149–182. DOI: 10.1016/j.progpolymsci.2003.08.003

19. E. G. Rochow, *Silicon and Silicones*, Springer, Berlin, Heidelberg, New York, **1987**.

20. K. Fuchise, K. Sato, M. Igarashi, *Macromolecules* **2021**, *54*, 5204–5217. DOI: 10.1021/acs.macromol.0c02653

21. I. Krizhanovskiy, M. Temnikov, Y. Kononevich, A. Anisimov, F. Drozdov, A. Muzafarov, *Polymers*, **2022**, *14*, 3079. DOI: 10.3390/polym14153079

22. F. A. D. Herz, M. Nobis, D. Wendel, P. Pahl, P. J. Altmann, J. Tillmann, R. Weidner, S. Inoue, B. Rieger, *Green Chem.*, **2020**, *22*, 4489–4497. DOI: 10.1039/d0gc00272k

23. R. Bui, M. A. Brook, *Adv. Funct. Mater.*, **2020**, *30*, 2000737. DOI: 10.1002/adfm.202000737

24. Y. Nakajima, S. Shimada, *RSC Adv.*, **2015**, *5*, 20603–20616. DOI: 10.1039/C4RA17281G

25. R. J. Hofmann, M. Vlatkovic, F. Wiesbrock, *Polymers*, **2017**, *9*, 534. DOI: 10.3390/polym9100534

26. M. Tsumura, T. Iwahara, T. Hirose, *Polym. J.*, **1995**, *27*, 1048–1053. DOI: 10.1295/polymj.27.1048

27. J. Hu, P. I. Carver, D. J. Meier, E. J. Stark, N. Xu, T. Zhang, C. Hartmann-Thompson, P. R. Dvornic, *Polymer*, **2012**, *53*, 5459–5468. DOI: 10.1016/j.polymer.2012.09.052

28. U. Will, D. Veljanovski, P. Härter, B. Rieger, *Macromolecules*, **2010**, *43*, 934–938. DOI: 10.1021/ma902425y

29. G. D. Sorarù, F. Dalcanale, R. Campostrini, A. Gaston, Y. Blum, S. Carturan, P. R. Aravind, *J. Mater. Chem.*, **2012**, *22*, 7676–7680. DOI: 10.1039/c2jm00020b

30. N. G. Vasilenko, E. A. Rebrov, A. M. Muzafarov, B. Eßwein, B. Striegel, M. Möller, *Macromol. Chem. Phys.*, **1998**, *199*, 889–895. DOI: 10.1002/(SICI)1521-3935(19980501)199:5<889::AID-MACP889>3.0.CO;2-T

31. A. M. Muzafarov, E. A. Tatarinova, N. V. Vasilenko, G. M. Ignat'eva, in: *Organosilicon Compounds. Experiment (Physico-Chemical Studies) and Applications*, Acad. Press, London, **2017**, ch. 7, pp. 323–382. DOI: 10.1016/B978-0-12-814213-4.00008-3

32. A. Morikawa, M. Kakimoto, Y. Imai, *Macromolecules*, **1992**, *25*, 3247–3253. DOI: 10.1021/ma00038a034

33. E. Yu. Katarzhnova, G. M. Ignatyeva, A. A. Kalinina, E. V. Talalaeva, A. S. Tereshchenko, *INEOS OPEN*, **2020**, *3*, 219–225. DOI: 10.32931/io2026a

34. M. Grzelak, R. Januszewski, B. Marciniec, *Inorg. Chem.*, **2020**, *59*, 7830–7840. DOI: 10.1021/acs.inorgchem.0c00947

35. H. Maciejewski, K. Szubert, B. Marciniec, *Catal. Commun.*, **2012**, *24*, 1–4. DOI: 10.1016/j.catcom.2012.03.011

36. B. Müller, W. Rath, *Formulating Adhesives and Sealants*, Vincentz Network, Hanover, **2010**. DOI: 10.1515/9783748602279

37. F. de Buyl, *Int. J. Adhes. Adhes.*, **2001**, *21*, 411–422. DOI: 10.1016/S0143-7496(01)00018-5

38. S. C. Shit, P. Shah, *Natl. Acad. Sci. Lett.*, **2013**, *36*, 355–365. DOI: 10.1007/s40009-013-0150-2

39. C. D. Weber, C. Bradley, M. C. Lonergan, *J. Mater. Chem. A*, **2014**, *2*, 303–307. DOI: 10.1039/c3ta14132b

40. A. M. Bueche, *J. Polym. Sci.*, **1955**, *15*, 105–120. DOI: 10.1002/pol.1955.120157909

41. M. L. Dunham, D. L. Bailey, R. Y. Mixer, *Ind. Eng. Chem.*, **1957**, *49*, 1373–1376. DOI: 10.1021/ie50573a029

42. D. Bodas, J.-Y. Rauch, C. Khan-Malek, *Eur. Polym. J.*, **2008**, *44*, 2130–2139. DOI: 10.1016/j.eurpolymj.2008.04.012

43. L. Xue, Y. Zhang, Y. Zuo, S. Diao, J. Zhang, S. Feng, *Mater. Lett.*, **2013**, *106*, 425–427. DOI: 10.1016/j.matlet.2013.05.084

44. S. Walker, U. Daalkhaijav, D. Thrush, C. Branyan, O. D. Yirmibesoglu, G. Olson, Y. Menguc, *3D Print. Addit. Manuf.*, **2019**, *6*, 139–147. DOI: 10.1089/3dp.2018.0117

45. A. Unkovskiy, S. Spintzyk, J. Brom, F. Huettig, C. Keutel, *J. Prosthet. Dent.*, **2018**, *120*, 303–308. DOI: 10.1016/j.prosdent.2017.11.007

46. L.-y. Zhou, Q. Gao, J.-z. Fu, Q.-y. Chen, J.-p. Zhu, Y. Sun, Y. He, *ACS Appl. Mater. Interfaces*, **2019**, *11*, 23573–23583. DOI: 10.1021/acsami.9b04873

47. J. Stieghorst, T. Doll, *Addit. Manuf.*, **2018**, *24*, 217–223. DOI: 10.1016/j.addma.2018.10.004

48. A. Hahn, G. Brandes, P. Wagener, S. Barcikowski, *J. Controlled Release*, **2011**, *154*, 164–170. DOI: 10.1016/j.jconrel.2011.05.023

49. J. Davies, C. S. Nunnerley, A. C. Brisley, J. C. Edwards, S. D. Finlayson, *J Colloid Interface Sci.*, **1996**, *182*, 437–443. DOI: 10.1006/jcis.1996.0485

50. D. G. Blackmond, *Angew. Chem., Int. Ed.*, **2005**, *44*, 4302–4320. DOI: 10.1002/anie.200462544

51. M. Brendel, D. Bonvin, W. Marquardt, *Chem. Eng. Sci.*, **2006**, *61*, 5404–5420. DOI: 10.1016/j.ces.2006.04.028

52. M. Gómez-Gallego, M. A. Sierra, *Chem. Rev.*, **2011**, *111*, 4857–4963. DOI: 10.1021/cr100436k

53. A. S. Tomlin, T. Turányi, *Analysis of Kinetic Reaction Mechanisms*, Springer, Berlin, Heidelberg, **2014**. DOI: 10.1007/978-3-662-44562-4

54. D. L. Sparks, D. L. Suarez, *Rates of Soil Chemical Processes*, Soil Sci. Soc. Am., Madison, **1991**.

55. J. Wei, J. L. Anderson, K. B. Bischoff, J. H. Seinfeld, in: *Detailed Chemical Kinetic Modeling: Chemical Reaction Engineering of the Future*, *Adv. Chem. Eng.*, Acad. Press, **1992**, vol. 18.

56. R. Y. Lukin, A. M. Kuchkaev, A. V. Sukhov, G. E. Bekmukhamedov, D. G. Yakhvarov, *Polymers*, **2020**, *12*, 2174. DOI: 10.3390/polym12102174

57. A. K. Roy, *Adv. Organomet. Chem.*, **2007**, *55*, 1–59. DOI: 10.1016/S0065-3055(07)55001-X

58. L. N. Lewis, J. Stein, Y. Gao, R. E. Colborn, G. Hutchins, *Platinum Met. Rev.*, **1997**, *41*, 66–75. DOI: 10.1595/003214097X4126675

59. A. J. Chalk, J. F. Harrod, *J. Am. Chem. Soc.*, **1965**, *87*, 16–21. DOI: 10.1021/ja01079a004

60. A. V. Radchenko, F. Ganachaud, *Ind. Eng. Chem. Res.*, **2022**, *61*, 7679–7698. DOI: 10.1021/acs.iecr.2c01015

61. I. K. Goncharova, S. A. Filatov, A. P. Drozdov, A. A. Tereshchenko, P. A. Knyazev, A. A. Guda, I. P. Beletskaya, A. V. Arzumanyan, *J. Catal.*, **2024**, *429*, 115269. DOI: 10.1016/j.jcat.2023.115269

62. E. Yu. Katarzhnova, G. M. Ignat'eva, E. A. Tatarinova, *INEOS OPEN*, **2022**, *5*, 113–129. DOI: 10.32931/io2224r

63. I. K. Goncharova, R. A. Novikov, I. P. Beletskaya, A. V. Arzumanyan, *J. Catal.*, **2023**, *418*, 70–77. DOI: 10.1016/j.jcat.2023.01.004

64. D. Troegel, J. Stohrer, *Coord. Chem. Rev.*, **2011**, *255*, 1440–1459. DOI: 10.1016/j.ccr.2010.12.025

65. H. Brunner, *Angew. Chem., Int. Ed.*, **2004**, *43*, 2749–2750. DOI: 10.1002/anie.200301742

66. A. K. Roy, R. B. Taylor, *J. Am. Chem. Soc.*, **2002**, *124*, 9510–9524. DOI: 10.1021/ja0127335

67. J. Stein, L. N. Lewis, Y. Gao, R. A. Scott, *J. Am. Chem. Soc.*, **1999**, *121*, 3693–3703. DOI: 10.1021/ja9825377

68. P. Cancouët, S. Pernin, G. Hélary, *J. Polym. Sci, Part A: Polym. Chem.*, **2000**, *38*, 837–845. DOI: 10.1002/(SICI)1099-0518(20000301)38:5<837::AID-POLA8>3.0.CO;2-2

69. D. A. de Vekki, V. A. Ol'sheev, V. N. Spevak, N. K. Skvortsov, *Russ. J. Gen. Chem.*, **2001**, *71*, 1912–1923. DOI: 10.1023/A:1014292310639

70. B. Marciniec, H. Maciejewski, W. Duczmal, R. Fiedorow, D. Kityński, *Appl. Organomet. Chem.*, **2003**, *17*, 127–134. DOI: 10.1002/aoc.402

71. Y. Qiong, Y. Hong, *Chin. J. Chem. Eng.*, **2006**, *14*, 555–558. DOI: 10.1016/S1004-9541(06)60115-8

72. N. C. Imlinger, M. Krell, M. R. Buchmeiser, *Monatsh. Chem.*, **2007**, *138*, 285–291. DOI: 10.1007/s00706-007-0619-0

73. O. Mukbaniani, T. Tatrishvili, G. Titvinidze, S. Patsatsia, *J. Appl. Polym. Sci.*, **2009**, *114*, 892–900. DOI: 10.1002/app.30530

74. G. Rajesh, P. K. Maji, M. Bhattacharya, A. Choudhury, N. Roy, A. Saxena, A. Bhowmick, *Polym. Polym. Compos.*, **2010**, *18*, 477–488. DOI: 10.1177/096739111001800902

75. T. K. Meister, K. Riener, P. Gigler, J. Stohrer, W. A. Herrmann, F. E. Kühn, *ACS Catal.*, **2016**, *6*, 1274–1284. DOI: 10.1021/acscatal.5b02624

76. A. Dietrich, E. Mejía, *Eur. Polym. J.*, **2020**, *122*, 109377. DOI: 10.1016/j.eurpolymj.2019.109377

77. W. Müller, A. Wöhl, S. Peitz, N. Peulecke, B. R. Aluri, B. H. Müller, D. Heller, U. Rosenthal, M. H. Al-Hazmi, F. M. Mosa, *ChemCatChem*, **2010**, *2*, 1130–1142. DOI: 10.1002/cctc.201000052

78. S. J. Dünki, F. A. Nüesch, D. M. Opris, *J. Mater. Chem. C*, **2016**, *4*, 10545–10553. DOI: 10.1039/c6tc01731b

79. T. Jalkanen, *Thermochim. Acta*, **2021**, *703*, 178982. DOI: 10.1016/j.tca.2021.178982

80. S. Vyazovkin, *Isoconversional Kinetics of Thermally Stimulated Processes*, Springer, Cham, **2015**. DOI: 10.1007/978-3-319-14175-6

81. G. Pan, C. Hu, S. Hong, H. Li, D. Yu, C. Cui, Q. Li, N. Liang, Y. Jiang, L. Zheng, L. Jiang, Y. Liu, *Nat. Commun.*, **2021**, *12*, 64. DOI: 10.1038/s41467-020-20233-w

82. V. L. Michaelis, M. L. Menten, *Biochem. Ztg.*, **1913**, *49*, 333–369.

83. K. A. Johnson, R. S. Goody, *Biochemistry*, **2011**, *50*, 8264–8269. DOI: 10.1021/bi201284u

84. J. L. Lortie, T. Dudding, B. M. Gabidullin, G. I. Nikonov, *ACS Catal.*, **2017**, *7*, 8454–8459. DOI: 10.1021/acscatal.7b02811

85. M. V. Dobrynin, C. Pretorius, D. V. Kama, A. Roodt, V. P. Boyarskiy, R. M. Islamova, *J. Catal.*, **2019**, *372*, 193–200. DOI: 10.1016/j.jcat.2019.03.004

86. A. Tahara, H. Nagashima, *Tetrahedron Lett.*, **2020**, *61*, 151423. DOI: 10.1016/j.tetlet.2019.151423

87. X. Du, Z. Huang, *ACS Catal.*, **2017**, *7*, 1227–1243. DOI: 10.1021/acscatal.6b02990

88. Y. Toya, K. Hayasaka, H. Nakazawa, *Organometallics*, **2017**, *36*, 1727–1735. DOI: 10.1021/acs.organomet.7b00087

89. M. Zhang, A. Zhang, *Appl. Organomet. Chem.*, **2010**, *24*, 751–757. DOI: 10.1002/aoc.1701

90. J. Sun, L. Deng, *ACS Catal.*, **2016**, *6*, 290–300. DOI: 10.1021/acscatal.5b02308

91. C. Darcel, J.-B. Sortais, D. Wei, A. Bruneau-Voisine, in: *Non-Noble Metal Catalysis: Molecular Approaches and Reactions*, R. J. M. Klein Gebbink, M.-E. Moret (Eds.), Wiley, Weinheim, **2019**, ch. 10, pp. 241–264. DOI: 10.1002/9783527699087.ch10

92. X. Yang, C. Wang, *Chem. Asian J.*, **2018**, *13*, 2307–2315. DOI: 10.1002/asia.201800618

93. D. E. Pérez, J. L. Smeltz, R. D. Sommer, P. D. Boyle, E. A. Ison, *Dalton Trans.*, **2017**, *46*, 4609–4616. DOI: 10.1039/c7dt00271h

94. O. V. Novozhilov, I. V. Pavlichenko, N. V. Demchenko, A. I. Buzin, N. G. Vasilenko, A. M. Muzafarov, *Russ. Chem. Bull.*, **2010**, *59*, 1909–1917. DOI: 10.1007/s11172-010-0332-8

95. L. Liu, X. Li, Y. Ma, C. Wu, G. Han, *Kinet. Catal.*, **2020**, *61*, 414–420, DOI: 10.1134/S0023158420030167

96. A. S.-m. Chang, K. E. Kawamura, H. S. Henness, V. M. Salpino, J. C. Greene, L. N. Zakharov, A. K. Cook, *ACS Catal.*, **2022**, *12*, 11002–11014. DOI: 10.1021/acscatal.2c03580

97. V. P. Ananikov, K. A. Gayduk, I. P. Beletskaya, V. N. Khrustalev, M. Y. Antipin, *Eur. J. Inorg. Chem.*, **2009**, 1149–1161. DOI: 10.1002/ejic.200800984

98. A. S. Galushko, V. V. Ilyushenkova, J. V. Burykina, R. R. Shaydullin, E. O. Pentsak, V. P. Ananikov, *Inorganics*, **2023**, *11*, 260. DOI: 10.3390/inorganics11060260

99. M. A. Guseva, D. A. Alentiev, E. V. Bermesheva, I. A. Zamilatskov, M. V. Bermeshev, *RSC Adv.*, **2019**, *9*, 33029–33037. DOI: 10.1039/C9RA06784A